

Study of Possible Local Quasars and Search for a Quasar-Stellar Connection. III. A Sample of 341 QSOs

Kiril P. Panov*

Institute of Astronomy and National Astronomical Observatory, Bulgarian Academy of Sciences, Sofia, Bulgaria

Abstract. A new sample of 341 possible local QSOs are presented, which are in the vicinity of low redshift galaxies. Physical characteristics of the sample quasars are determined and previously reported relations are confirmed: density - redshift, absolute mag - radius, absolute mag - mass, mass - radius, mass - luminosity, and mass - density. These relations seem to support the basic assumptions that quasars are single, compact objects, with dimensions close to their respective gravitational radius. Redshifts of quasars are dominated by a gravitational redshift component, and the gravitational redshifts seem to be quantized according to the Karlsson - sequence. Evidence is found in favour of the Arp's evolutionary scenario: QSOs are ejected from their respective parent galaxy and evolve as they recede, building new small mass companion galaxies. Evidence is found that in the course of evolution the quasar density and redshift decrease, while dimensions and luminosity increase. Relation luminosity - density is found in the sense that more dense quasars are less luminous.

Simple linear density equation is found, which seems to apply to quasars, but also to stars and may be even to planets, providing a possible link between these seemingly very different structures in the Universe. Evidence is found of possible increase of quasar mass and luminosity with increasing distance to about $z=0.03$. The physics behind all these processes and relations remain unclear, but a revival of the old Ambartsumian's hypotheses seems possible, suggesting disintegration of an unknown primordial dense matter. The properties of quasars may invoke the need for deeper changes in our current theories. Most fascinating seems the possibility that a link may exist between quasars and stars.

Keywords: Active galaxies, Quasars, Gravitational redshifts, Evolution of quasars.

1. INTRODUCTION

The study of quasars is a most fascinating part of modern astrophysics and may have direct implications for our fundamental knowledge about the origin of galaxies. The standard theory about origin of galaxies is based on a gravitational collapse onto some previously built kernels. How these kernels were built in an expanding Universe (even inflationary expanding at the beginning) is still an open question. During the last decades, new ideas have been proposed, and which are radically deviating from conventional theories.

The origin of these unconventional ideas is the interpretation of quasar redshifts as non-cosmological. According to the Standard Quasar Model (SQM), most popular at present, the unprecedented large quasar redshifts are caused by the expansion of the Universe [1-3]. Assuming that quasars are at cosmological distances has an immediate consequence - quasars have to be extremely luminous. According to the SQM quasars are huge black holes accreting matter [1-3]. Not only are the quasars' luminosities huge, but it also seems, judging by their visual magnitudes that with increasing cosmological distances quasar luminosity should increase [4, 5]. On the face of it, such a conclusion could raise doubts. This problem needs, however, further consideration.

In the SQM, quasars are the most distant objects in the Universe, because of their large redshifts. There is a disturbing fact from the beginning, however - quasars do not follow the Hubble relation found for galaxies. How can we be sure we could apply the Hubble relation to determine the distances for quasars? A possible outcome of this problem may be the large spread of quasar luminosities. Although this may or may not be the real explanation of the problem, we should keep in mind the simple fact that quasars do not obey the Hubble relation, and a different cause for that may also exist.

Already during the first years after their discovery, attempts have been made to explain the quasar redshifts in different, "non-cosmological" ways. Among the most debated are the ideas based on the "intrinsic" origin of the redshifts: gravitational reddening [6-8], and the "variable mass hypothesis" [9, 10]. The debate between the SQM and the "intrinsic-origin" hypothesis continues for more than 40 years, to this present day. If the redshifts of quasars are caused by intrinsic origin, the quasars are probably of local origin - local quasars. Both the SQM and the "intrinsic" views have their observational support and weak points. Strong observational support for the SQM comes from the observations of quasars hosted by galaxies, where in a few cases the redshift of the "hosted" quasar and that of the "hosting" galaxy are identical [11, 12]. However, one should be aware of the observing difficulties and the possibility of "contamination" by quasar light when the hosting galaxy is observed. Moreover, there is at least one reported case,

*Address correspondence to this author at the Institute of Astronomy and National Astronomical Observatory, Bulgarian Academy of Sciences, Sofia, Bulgaria; Tel: 974 1910; Fax: 974 1910; E-mail: kpanov@astro.bas.bg

where quasar of $z = 2.114$ was found very close to the nucleus of the galaxy NGC 7319 with $z = 0.022$ [13]. Clearly, the above argument can not be used by either side of this controversy, before further research work will have been done. There are a number of questions that the SQM leaves unanswered, or at least, not satisfactorily answered. I already mentioned the seemingly increasing quasar luminosity with the cosmological distance. There is also the question, why is the number of observed QSOs with $z > 3$ decreasing? The number of quasars at larger cosmological distances is expected to increase and there has to be a reason for not seeing them. There is an interesting problem that concerns all hypothesis proposed for quasars - the Karlsson sequence of quasars redshifts. This is a sequence of specific and preferred redshifts for QSOs: 0.06, 0.30, 0.60, 0.96, 1.41, 1.96, and so on. The sequence could be obtained by: $\Delta \log(1+z) = 0.089$ [14-17]. The Karlsson sequence was found with the early surveys of quasars but later not confirmed with modern redshift catalogues. On the face of it, this looks like a preliminary finding has been discarded by later, larger samples of data. For the SQM such an interpretation would be a relief. If confirmed, the Karlsson sequence would require (in the SQM) that the Universe should be expanding in shells of different and specific velocity values and that would be inconceivable. This sequence is a major obstacle also for the local origin hypothesis of quasars. In the framework of the gravitational reddening hypothesis an outcome could be found but only at a cost of a major sacrifice: a departure from a basic physical concept [18]. This will be discussed below. However, before we try to find an explanation of the Karlsson sequence, we have to answer the question, is the Karlsson sequence real? If it is, why modern surveys could not confirm it?

Quasars release huge amount of energy. With the SQM, these energies have to be as large as $\sim 10^{45}$ ergs/s in a lifetime of $\sim 10^7 - 10^8$ years. In the framework of the gravitational reddening hypothesis, the energies released by local quasars have to be $\sim 10^{39} - 10^{42}$ ergs/s [18]. How is this enormous energy output produced? In the SQM, the “engine” is provided by accretion onto a huge black hole. The local quasar model has as yet no specific physical engine. All we could say at this point is that the known physical processes are probably not sufficient to explain the quasar energy output.

The local quasar concept has also observational support. Since many years ago, researchers reported the association of high redshift QSOs with low redshift galaxies [19-30]. In some “discordant redshift associations”, as Halton Arp calls them [19], there may be seen filaments, connecting the high redshift quasar with the low redshift galaxy. Prominent examples are NGC4319 and Mk205 [31], NGC3067 and 3C232 [32, 33] etc. In other cases, quasars have been found very close to a low redshift galaxy [13, 34]. Considerations show that a chance projection in these cases has a very low probability, $\sim 10^{-8}$ and lower [35, 36]. Even large groups of quasars have been reported clustering around low redshift galaxies [37-41]. All these findings lead to the conclusion that quasars around low redshift active galaxies have been ejected by the respective parent galaxy [42-46].

Taking the same distance for a group of QSOs, as for their parent galaxy, it is possible to obtain some of the qua-

sars’ physical characteristics [18]. One more observational result should be mentioned, and which remains, in my opinion, a mystery for all proposed quasar models. If QSOs are the most distant objects in the Universe (according to SQM), they also have to be most young. One should expect that quasars are deficient in metals and a gradient of the metal abundances should exist in the sense that most distant quasars (largest redshifts) are most metal deficient. Surprisingly, high metal abundances were found in high redshift QSOs and no metal-gradient with distance so far has been claimed [47-49]. What do these findings mean, if confirmed? Are metals produced by rapidly evolved stellar populations around quasars, so soon after the Big Bang? Or, may be, yet another quasar riddle? This difficulty remains also for the gravitational reddening model, based on the disintegration of dense matter. Do we need to consider the possibility of an unknown process producing metals in a different way? The only way known to produce heavy elements at present are nuclear processes in stars, at late stages of their evolution. Especially interesting would be to look for a gradient of the metal abundances from higher to lower redshifts.

Some quasars exhibit jets of yet unknown nature (e.g. 3C345 in the vicinity of NGC6212). In some cases, moving structures were found by radio-observations along these jets [50, 51]. If quasars are at cosmological distances, the velocities of these moving structures should be super-luminous. On the other hand, if quasars and their jets are of local origin (e.g. 3C345 would be at about the same distance as NGC6212), the “super-luminous” velocities will be reduced below the velocity of light. In the case of 3C345 this velocity would be reduced to $0.33 c$ [52].

Most decisive observations that can in principle distinguish between the “cosmological” and the “local” origin of quasars are observations of host galaxies.

During the last years, there are an increasing number of studies of host galaxies [53-58] which suggests that a solution of this problem in near future is possible.

In this paper, important astrophysical questions will be addressed and some tantalizing answers will be suggested. In the following I will use the procedure, outlined in [18, 59] to determine physical characteristics of a sample of 116 possible local quasars. These are added to the already published data [59] to build a sample of 341 possible local QSOs, and which are used to study relations for quasars. The sample of all 341 quasars studied is listed in Table I.

2. DETERMINATION OF PHYSICAL CHARACTERISTICS OF LOCAL QUASARS.

Assuming that the clustering of quasars around some active galaxies is real, as researchers claim, we could obtain some of the physical characteristics of QSOs [18, 59]. In these cases, it is possible to take for a group of quasars near an active galaxy the distance of the parent galaxy. The observed quasar redshift could be taken as composed by three components of different origin, according to Burbidge [60]:

$$(1 + z_o) = (1 + z_c) \cdot (1 + z_{gr}) \cdot (1 + z_d) \quad (1)$$

In eq (1), z_o is the observed redshift, z_c is the cosmological redshift, z_{gr} is the intrinsic redshift, specified here as gravitational redshift, and z_d is the Doppler shift. As men-

Table 1. Sample of 341 Local Quasars (Data from Veron-Cetty and Veron, 2010, 13 th ed.)

Galaxy Redshift	Quasar	Redshift Z_0	Visual mag	B-V	References
NGC0007 0.005	Q1= 2QZJ000827-2954	2.062	19.53	-	[62]
	Q2= 2QZJ000826-2957	2.041	20.74	-	
	Q3 2QZJ000802-2956	1.591	20.23	-	
NGC450 0.006	Q1= Q0107+0022	1.968	18.89	0.21	[37]
	Q2= Q0107-0235	0.958	17.80	-	
	Q3 Q0107-0232	0.728	18.85	-	
	Q4 PB6291	0.956	17.60	-	
	Q5 Q0107-025c	1.893	19.45	-	
	Q6 NGC450 No24	0.070	18.90	-	
	Q7 Q0107-001	0.468	19.38	0.09	
	Q8 Q0108-007	1.424	19.23	0.50	
	Q9 Q0108+0028	2.005	18.25	-	
	Q10 Q0108-025	1.240	18.10	-	
	Q11 Q0108-020	1.302	19.60	-	
	Q12 Q0108+001	1.003	18.67	0.26	
	Q13 Q0109-0128	1.758	18.37	0.26	
	Q14 Q0110-0107	1.896	19.29	0.22	
	Q15 Q0110-0157	1.102	17.30	-	
	Q16 PB6317	0.238	17.85	0.28	
	Q17 Q0110+004	0.910	20.08	0.21	
	Q18 Q0110-0015	0.976	18.55	-	
	Q19 Q0110-030	1.235	17.70	-	
	Q20 Q0110-0047	0.412	19.06	0.29	
	Q21 Q0110-006	0.935	19.70	-	
	Q22 Q0111-007	0.995	18.63	0.28	
	Q23 Q0111-008	0.181	18.93	0.58	
	Q24 Q0111-010	0.350	19.02	0.33	
	Q25 Q0111-005	1.908	19.45	-	
	Q26 PKS0112-017	1.365	17.50	-	
	Q27 Q0112-012	1.585	19.89	0.20	
	Q28 Q0113+000	1.279	19.19	0.37	
	Q29 Q0113-010	1.968	19.58	0.20	
	Q30 Q0113-013	2.055	19.60	-	
	Q31 Q0113-009	1.263	18.96	0.36	
	Q32 Q0114-001	1.316	18.94	0.35	

Table 1. contd...

Galaxy Redshift	Quasar	Redshift Z_0	Visual mag	B-V	References
	Q33 UM314	2.190	18.32	0.22	
	Q34 UM315	2.050	18.70	-	
	Q35 Q0116-010	1.052	18.60	0.32	
	Q36 NGC450 No86	0.090	17.35	0.44	
	Q37 Q0117-023	2.019	19.80	-	
	Q38 Q0117+001	0.649	19.30	0.17	
	Q39 UM316	0.960	17.90	-	
	Q40 Q0117-012	0.202	19.13	0.65	
	Q41 NGC450 No87	0.078	19.45	-	
	Q42 Q0118-031A	1.445	18.35	-	
	Q43 Q0118-018	1.911	19.45	-	
	Q44 PB8737	1.165	18.45	-	
	Q45 PB8736	2.112	19.00	-	
	Q46 Q0118+003	0.328	19.11	0.28	
	Q47 NGC450 No217	0.135	18.75	-	
	Q48 Q0119-009	1.943	19.30	0.20	
	Q49 Q0120-001	0.909	19.21	0.37	
	Q50 Q0120-029A	1.073	18.55	-	
	Q51 Q0120-002	1.355	19.01	0.45	
	Q52 Q0120-029B	0.438	18.10	-	
	Q53 Q0120+002	0.772	19.25	-	
	Q54 Q0121+007	1.310	19.60	-	
	Q55 Q0121+009	1.555	19.04	0.33	
	Q56 Q0121-008	2.252	19.30	-	
	Q57 Q0121+008	2.043	19.50	-	
	Q58 Q0121-022	0.988	19.05	-	
	Q59 Q0122-028	2.022	19.50	-	
	Q60 Q0123-005A	1.889	19.00	-	
	Q61 Q0123-005B	1.763	18.90	0.26	
	Q62 UM322	1.930	18.40	-	
	Q63 UM324	0.355	17.35	-	
NGC470 0.008	Q1=NGC470.68D	1.533	18.50	-	[63]
	Q2 =NGC470.68	1.875	19.80	-	
NGC520 0.008	Q1=NGC520.D9	1.670	18.60	-	[64]
	Q2 =NGC520.D2	0.311	18.90	-	

Table 1. contd...

Galaxy Redshift	Quasar	Redshift Z_0	Visual mag	B-V	References
	Q3 NGC520.192	2.000	20.20	-	
	Q4 NGC520.D5	1.609	19.80	-	
	Q5 NGC520.D8	2.090	19.30	-	
	Q6 NGC520.57	1.902	19.20	-	
NGC613 0.005	Q1 = 2QZJ013356-2922	2.222	20.09	-	[65]
	Q2 = 2QZJ013445-2928	2.059	20.32	-	
	Q3 2QZJ013454-2925	2.062	20.01	-	
	Q4 2QZJ013348-2920	1.855	20.30	-	
	Q5 2QZJ013345-2917	1.413	20.50	-	
	Q6 2QZJ013508-2930	1.482	20.31	-	
NGC622 0.017	Q1 = NGC622 UB1	0.910	18.36	0.32	[66]
	Q2 = NGC622 BS01	1.460	19.13	0.20	
NGC936 0.005	Q1 = PKS0225-014	2.042	18.60	-	[65, 67]
	Q2 = SDSSJ02274-0106	2.176	18.84	0.37	
	Q3 NGC936UB1	1.130	19.13	0.30	
NGC1068 0.003	Q1 = RXSJ02393-0001	0.261	15.48	0.30	[68]
	Q2 = Q0238-0001	0.468	19.07	0.24	
	Q3 Q0238-0058	0.726	18.52	0.19	
	Q4 Q0239-0008	0.649	18.72	0.12	
	Q5 Q0239+0021	1.054	18.92	0.30	
	Q6 Q0239-0005	1.552	18.47	0.25	
	Q7 Q0239-0012	1.112	18.70	0.00	
	Q8 1WGAJ0242.1+0000	0.385	19.67	0.31	
	Q9 Q0240-0012	2.018	18.45	0.28	
	Q10 Q0241+0005	0.684	18.92	0.17	
	Q11 1WGAJ0245.5-0007	0.655	18.91	0.09	
	Q12 1WGA 0242.6+0022	0.630	20.33	0.03	
	Q13 US3137	1.139	18.44	0.34	
	Q14 US3139	1.292	18.75	0.41	
	Q15 US3146	1.815	18.63	0.19	
	Q16 Q0244-0015	2.315	20.16	0.20	
NGC1073 0.004	Q1 = NGC1073U2	0.601	19.00	-	[69, 70]
	Q2 = PKS0241+011	1.400	20.30	-	

Table 1. contd...

Galaxy Redshift	Quasar	Redshift Z_0	Visual mag	B-V	References
	Q3 NGC1073U1	1.941	19.60	-	
	Q4 US3115	0.546	19.18	0.13	
NGC1097 0.004	Q2 = Q0238-315	2.143	19.60	-	[38]
	Q3 = Q0238-301	2.265	18.30	-	
	Q6 Q0238-310	2.034	19.50	-	
	Q7 Q0240-309	0.374	18.50	-	
	Q9 Q0241-316	1.588	19.90	-	
	Q10 Q0241-302	0.359	19.50	-	
	Q12 Q0242.0-3104	0.874	19.10	-	
	Q13 Q0242.1-3104	1.985	19.60	-	
	Q14 Q0242-305	1.045	18.80	-	
	Q15 Q0242.9-3010	2.269	19.90	-	
	Q16 Q0242.9-3009	0.783	19.60	-	
	Q18 Q0243.5-2946	1.577	20.20	-	
	Q19 Q0243.6-2947	2.063	20.10	-	
	Q20 Q0243-308	0.088	20.00	-	
	Q21 Q0243-318	1.875	18.50	-	
	Q23 QN1097.3	1.000	17.50	-	
	Q24 QN1097.4	0.340	18.20	-	
	Q25 QN1097.6	1.100	20.50	-	
	Q26 QN1097.5	0.887	20.00	-	
NGC2639 0.011	Q1 = NGC2639U1	1.177	18.06	0.29	[43] [71]
	Q2 = NGC2639U2	1.105	19.16	0.36	
	Q3 NGC2639U3	1.522	19.43	0.33	
	Q4 NGC2639U4	0.780	18.87	0.49	
	Q5 NGC2639U5	1.494	17.92	0.55	
	Q7 NGC2639U7	2.000	19.37	0.37	
	Q8 NGC2639U8	2.800	19.00	0.32	
	Q10 NGC2639U10	0.305	17.80	0.22	
	Q14 NGC2639U14	2.124	18.74	0.31	
	Q15 NGC2639U15	1.525	18.78	0.22	
	Q16 NGC2639 No3	0.323	18.40	0.17	
NGC2683 0.0014	Q1= NGC2683U3	1.252	19.04	0.31	[72]
	Q2 =NGC2683U2	1.262	19.65	0.55	

Table 1. contd...

Galaxy Redshift	Quasar	Redshift Z_0	Visual mag	B-V	References
	Q3 NGC2683U8	0.065	18.60	-	
	Q4 NGC2683U1	0.621	17.79	0.15	
NGC2841 0.0021	Q1= NGC2841UB2	0.120	18.70	-	[73]
	Q2 =NGC2841UB1	2.028	19.28	0.21	
NGC2859 0.0056	Q1= NGC2859U1	0.230	18.74	0.41	[74]
	Q2 =NGC2859U2	2.250	19.70	-	
	Q3 NGC2859U3	1.460	20.30	-	
	Q6 NGC2859U6	0.027	18.50	-	
NGC2916 0.0124	Q1= NGC2916UB5	1.546	19.23	0.35	[73]
	Q2 =NGC2916UB1	0.238	19.20	-	
	Q3 NGC2916UB2	0.793	19.00	-	
	Q4 NGC2916UB4	1.868	19.35	0.13	
	Q5 NGC2916UB3	1.279	19.09	0.43	
NGC3034 0.001	= M82 Q1 = M82 No95	1.010	19.44	0.36	[75]
	Q2 = Hoag 1	2.048	19.50	0.30	
	Q3 Hoag 2	2.054	20.33	0.22	
	Q4 NGC3031U4	0.85	20.12	0.70	
	Q5 Hoag 3	2.040	20.31	0.16	
	Q6 Bol 105	2.240	21.40	-	
	Q7 M82 No69	0.930	19.38	0.70	
	Q8 M82 No22	0.960	19.04	1.31	
	Q9 Bol 75	0.740	22.00	-	
	Q10 Dahlem 7	0.675	19.80	-	
	Q11 Dahlem 12	0.626	18.90	-	
	Q12 Dahlem 17	1.086	17.99	0.33	
NGC3079 0.004	Q1 = SBS0953+556	1.410	18.45	0.17	[76]
	Q2 = 4C55.17	0.898	17.89	0.35	
	Q3 SBS0955+560	1.021	17.68	0.47	
	Q4 RXJ10005+5536	0.215	19.37	0.62	
	Q5 1WGAJ1000.9+5541	1.037	19.99	0.57	
	Q6 NGC3073UB1	1.530	19.04	0.32	
	Q7 ASV1	0.072	17.28	-	
	Q8 SBS0957+557	2.102	17.60	-	

Table 1. contd...

Galaxy Redshift	Quasar	Redshift Z_0	Visual mag	B-V	References
	Q9 Q0957+561A	1.413	16.95	0.21	
	Q10 Q0957+561B	1.415	16.95	0.21	
	Q11 ASV24	1.154	23.03	-	
	Q12 ASV31	0.352	21.14	-	
	Q13 MARK132	1.760	16.05	0.28	
	Q14 NGC3073UB4	1.154	18.38	0.38	
	Q15 1WGAI1002.7+5558	0.219	21.20	-	
	Q16 Q0958+5625	3.216	20.08	-	
NGC3184 0.002	Q1 = NGC3184UB4	0.675	18.23	0.13	[73]
	Q2 = NGC3184UB3	0.920	19.21	0.35	
	Q3 NGC3184UB1	0.152	17.70	-	
NGC3384 0.0023	Q1= NGC3384U1	0.442	19.31	0.19	[77]
	Q2 = NGC3384U2	1.280	19.27	0.34	
	Q4 NGC3384U4	1.107	19.06	0.25	
	Q5 NGC3384U5	1.192	20.00	-	
	Q8 NGC3384U8	1.134	18.56	0.45	
	Q13 NGC3384U13	0.497	19.57	0.43	
	Q14 NGC3384U14	0.520	19.94	0.21	
	Q15 NGC3384U15	1.131	19.76	0.44	
NGC3516 0.009	Q1= 1WGAI1107.7+7232	2.100	18.50	-	[78]
	Q2 =1WGAI1105.4+7238	1.399	20.00	-	
	Q3 1WGAI1105.1+7242	0.930	20.00	-	
	Q4 1WGAI1106.2+7244	0.690	19.10	-	
	Q5 1WGAI1108.5+7226	0.328	20.20	-	
	Q6 NGC3516U2	1.710	18.60	-	
NGC3628 0.003	Q1 = Wee 47	1.413	19.06	0.26	[39]
	Q2 = Wee 48	2.060	18.91	0.26	
	Q3 Wee 50	1.750	19.58	0.18	
	Q4 Wee 51	2.150	19.44	0.29	
	Q8 Wee 52	2.430	20.97	0.24	
	Q9 Wee 55	1.940	19.06	0.26	
	Q10 Wee 36	2.490	20.70	-	
	Q11 Wee 38	2.370	20.05	0.48	
	Q12 Wee 45	2.100	20.12	0.08	

Table 1. contd...

Galaxy Redshift	Quasar	Redshift Z_0	Visual mag	B-V	References
	Q13 Wee 37	2.140	20.02	0.55	
	Q14 Wee 40	1.740	20.09	0.13	
	Q15 Wee 34	2.320	17.85	0.65	
	Q16 Wee 46	0.060	20.20	-	
	Q17 Wee 41	2.540	20.02	0.25	
	Q18 Wee 44	2.380	19.57	0.25	
	Q19 Wee 42	2.110	20.97	0.16	
	Q20 Wee 43	3.009	19.83	0.33	
NGC3842 0.0211	Q1 = Q1141+2013	0.335	18.50	-	[79, 80]
	Q2 = Q1141+2014	0.946	19.08	0.24	
	Q3 Q1141+2012	2.200	20.18	0.25	
NGC4235 0.007	Q1 = PG1216+069	0.334	15.65	-	[71]
	Q2 = 1ES1212+078 (BL)	0.137	16.00	-	
NGC4258 0.002	Q1 = QJ1218+472	0.398	19.88	0.21	[42]
	Q2 = QJ1219+473	0.654	19.43	0.17	
NGC4410 0.025	Q1 = SDSSJ12260+0853	2.237	19.57	0.27	[40]
	Q2 = SDSSJ12260+0912	0.662	19.24	0.09	
	Q3 SDSSJ12255+0859	1.903	19.57	0.21	
	Q5 Q1222+0901	0.535	17.29	0.10	
	Q6 SDSSJ12273+0923	1.776	19.39	0.13	
	Q8 2E1225+0858	0.085	16.64	0.38	
	Q9 SDSSJ12281+0915	1.590	20.03	0.45	
	Q10 SDSSJ12279+0922	1.502	18.82	0.26	
	Q11 SDSSJ12261+0935	0.628	19.33	0.12	
	Q12 SDSSJ12238+0856	1.043	18.74	0.30	
	Q13 SDSSJ12235+0902	1.363	19.24	0.34	
	Q15 Q1225+0836	1.471	17.59	0.30	
	Q16 SDSSJ12178+0913	1.076	19.48	0.21	
	Q17 SDSSJ12240+0935	1.345	19.32	0.24	
	Q18 SDSSJ12230+0856	1.090	19.12	0.34	
	Q19 SDSSJ12231+0914	1.715	19.49	0.09	
	Q20 Q1220+0939	0.681	17.74	0.09	
	Q21 SDSSJ12291+0938	2.649	20.08	0.33	

Table 1. contd...

Galaxy Redshift	Quasar	Redshift Z_0	Visual mag	B-V	References
	Q22 SDSSJ12227+0853	0.773	18.78	0.15	
	Q23 SDSSJ12281+0951	0.064	17.72	0.65	
	Q24 Q1222+1010	0.398	18.58	0.12	
	Q25 SDSSJ12250+0955	1.429	19.04	0.26	
NGC4579 0.005	Q2 = Q1234+1217	0.662	18.61	0.11	[81]
NGC5548 0.017	Q1 = QJ14172+2534	0.852	18.40	-	[41]
	Q2 = EXO1415.2+2607	0.184	18.03	0.32	
	Q3 QJ14182+2500	0.727	18.90	-	
	Q4 Q1408.0+2696	2.425	19.08	0.20	
	Q5 Q1408.3+2626	2.100	20.22	0.52	
	Q6 Q1408.7+2665	1.928	18.74	0.22	
	Q7 FIRSTJ14162+2649	2.297	19.00	0.43	
	Q8 Q14144+256	1.800	20.50	0.18	
	Q9 Q14148+252	1.830	20.71	0.15	
	Q10 Q14149+251	1.917	18.86	0.22	
	Q11 2E1414+2513	1.057	19.50	0.46	
	Q12 1E14151+254	0.560	19.50	0.24	
	Q13 Q14151+254	2.310	19.57	0.35	
	Q14 HS1415+2701	2.500	17.70	0.46	
	Q15 2E1415+2557	0.237	17.20	0.80	
	Q16 2E1416+2523	0.674	18.70	-	
	Q17 HS1417+2547	2.200	18.10	0.52	
	Q18 KUV14189+2552	1.053	16.06	0.33	
	Q19 RXSJ14215+2408	0.084	17.27	0.30	
	Q20 PKS1423+24	0.649	17.26	0.36	
NGC5985 0.008	Q1 = SBS1537+595	2.125	19.00	0.14	[34]
	Q2 = SBS1535+596	1.968	18.66	0.29	
	Q3 HS1543+5921	0.807	17.63	0.28	
	Q4 SBS1532+598	0.690	17.57	0.19	
	Q5 SBS1549+590	0.348	17.42	0.21	
	Q6 SBS1533+588	1.895	18.39	0.19	
NGC6212 0.030	Q1=Q1636.8+3956	1.864	19.82	0.24	[52]
	Q2 = Q1636.9+4004	2.010	21.30	0.16	

Table 1. contd....

Galaxy Redshift	Quasar	Redshift Z_0	Visual mag	B-V	References
	Q3 Q1637.1+4008	1.898	19.63	0.43	
	Q4 Q1637.6+3910	0.461	17.43	0.29	
	Q5 FIRSTJ16395+3908	0.143	18.38	0.43	
	Q6 Q1638.0+3938	0.030	17.80	-	
	Q7 Q1638.2+4019	1.965	19.20	-	
	Q8 Q1638.8+4012	1.183	20.40	0.21	
	Q9 NRAO 512	1.666	19.37	-	
	Q10 Q1639.4+4006	2.253	19.08	0.19	
	Q11 Q1638.9+4002	1.625	18.60	0.19	
	Q12 Q1639.8+3940	2.614	19.09	0.16	
	Q13 MS16400+3940	0.540	19.83	0.18	
	Q14 2E1640+4007	1.005	18.05	0.24	
	Q15 Q1640.5+397	0.625	20.51	0.08	
	Q16 Q1640.8+401	2.529	20.32	0.34	
	Q17 Q1640.8+398	1.860	18.85	0.36	
	Q18 Q1640.9+4048	1.580	20.85	0.33	
	Q19 Q1640.9+401	1.595	19.62	0.26	
	Q20 Q1640.9+395	1.466	19.47	0.34	
	Q21 Q1640.0+397	1.414	20.00	0.33	
	Q22 SDSSJ16428+3924	2.384	19.27	0.22	
	Q23 3C345.0	0.595	16.59	0.22	
	Q24 Q1641.4+4049	1.360	18.24	0.26	
	Q25 Q1641.5+399	2.000	20.01	0.19	
	Q26 Q1641.6+4060	2.260	20.02	0.35	
	Q27 Q1641.6+398	2.000	20.82	0.27	
	Q28 Q1641.7+396	0.443	19.30	0.00	
	Q29 E1641.7+3998	0.704	18.32	0.12	
	Q30 Q1641.8+399	1.083	19.06	0.26	
	Q31 Q1641.9+401	2.113	19.31	0.24	
	Q32 E1641+399	0.594	19.50	0.06	
	Q33 Q1642.0+4015	1.358	18.55	0.36	
	Q34 Q1642.0+395	0.434	19.39	0.17	
	Q35 Q1642.6+400	1.377	19.45	0.30	
	Q36 Q1642.7+4016	0.608	19.13	0.02	
	Q37 Q1643.0+4006	1.268	19.31	0.51	
	Q39 Q1643.1+4062	1.451	19.04	0.17	
	Q40 Q1643.5+401	1.877	19.49	0.11	

Table 1. contd....

Galaxy Redshift	Quasar	Redshift Z_0	Visual mag	B-V	References
	Q41 Q1643.3+395	2.145	19.61	0.33	
	Q42 RXSJ16464+3929	0.100	17.60	0.24	
NGC6217 0.005	Q1 = 1WGAI1630.9+7810	0.358	20.60	-	[82]
	Q2 = 1WGAI1634.4+7809	0.376	20.80	-	
IC4553 = 0.018	Arp 220 Q1 = 1WGAI1533.8+2356	0.232	18.37	0.42	[83]
	Q2 = Q1532+2332 (Arp9)	1.249	19.82	-	
	Q3 1WGAI1535.0+2336	1.258	20.52	0.70	
	Q4 1WGAI1537.2+2300	0.463	19.20	0.12	
Mark231 0.042	Q1= 3C277.1	0.320	18.11	0.31	[84, 85]
	Q2= RXJ12548+5644	0.124	17.20	-	
	Q3 RXJ12549+5649	1.272	20.87	0.46	
	Q4 J12550+5649	1.232	19.76	0.33	
	Q5 J12554+5656	1.190	19.51	0.26	
	Q6 J13005+5728	0.330	18.83	0.18	
	Q7 SBS1258+569	0.072	17.35	0.28	
Mark273 0.037	Q1 = J13416+5514	0.207	18.46	0.85	[84, 85]
	Q2 = SBS1342+560	0.941	17.67	0.26	
	Q3 Mark273X	0.458	20.80	-	
	Q4 J1345.1+5547	1.166	18.78	0.36	
	Q5 J1346.0+5604	0.486	19.48	0.09	
	Q6 J13469+5607	0.377	19.45	0.36	
AM2230 -284 0.064	Q1 = 2QZJ223105-2926	2.141	19.93	-	[86]
	Q2 = 2QZJ223119-2816	2.152	20.67	-	
	Q3 2QZJ223155-2859	2.165	19.51	-	
	Q4 2QZJ223231-2818	2.161	20.15	-	
	Q5 2QZJ223233-2841	2.155	19.93	-	
	Q6 2QZJ223341-2807	2.134	20.49	-	
	Q7 2QZJ223337-2822	2.133	20.48	-	
	Q8 2QZJ223349-2909	2.154	20.33	-	
	Q10 2QZJ223426-2907	2.155	20.76	-	
	Q11 2QZJ223552-2811	2.136	20.39	-	
	Q12 2QZJ223716-2832	2.168	20.83	-	

Table 1. contd....

Galaxy Redshift	Quasar	Redshift Z_o	Visual mag	B-V	References
	Q13 2QZJ223755-2822	2.139	20.00	-	
	Q14 2QZJ223755-2901	2.137	20.36	-	

tioned above, the cosmological redshift for a quasar near a galaxy is taken to be the redshift of this (parent) galaxy. So far, only groups of QSOs around low redshift galaxies have been studied, and the redshifts of the parent galaxies are taken as cosmological. With the eq (1), one could try to answer the above question, why modern redshift surveys could not confirm the Karlsson sequence? Modern surveys could probably contain predominantly more distant and faint QSOs. Their cosmological redshifts, according to the eq. (1), contribute substantially to the observed redshift. In other words, if a specific pattern (e.g. the Karlsson sequence) exists in the gravitational redshifts, it would be impossible to detect it, if the quasar sample includes a large number of distant quasars. The absence of positive finding in this case does not necessarily mean that the Karlsson sequence does not exist - it could be undetectable. The contribution by the $(1 + z_d)$ term is also a “disturbing factor”, however, Doppler shifts should be limited, not depending on distance. The positive finding of the Karlsson sequence in early surveys could be true, after all.

In [18, 59], the following procedure has been adopted in order to decompose redshifts of QSOs. First, for all quasars of a group around a low redshift galaxy, the redshift of the galaxy (assumed cosmological) is taken out from each quasar’s observed redshift by:

$$z_i = (z_o - z_{gal}) / (1 + z_{gal}) \quad (2)$$

This procedure assumes that all quasars of a specific group are at about the same distance as their parent galaxy. Each z_i from eq (2) would now be composed by the gravitational and the Doppler component. As the projected Doppler component is limited (mostly less than 0.1 c, [59]), it seems possible to determine the gravitational reddening by simply comparing each z_i value with the Karlsson sequence and take the nearest value from that sequence as z_{gr} . Then the Doppler component could be decomposed by:

$$z_d = (z_i - z_{gr}) / (1 + z_{gr}) \quad (3)$$

In the following, assumptions will be made in order to determine physical characteristics of local quasars. Here is the summary:

- the sample consists of groups of quasars, spatially associated with respective low redshift (parent) galaxy, according to published studies (see Table 1);
- the observed redshift of each quasar is considered to be composed by three components, according to eq.(1);
- the cosmological redshift component of each quasar is taken to be the redshift of the respective parent galaxy;

- quasars are single bodies and they have a thermal outer layer;
- the intrinsic redshift is due to gravitational reddening and for local quasars it is the largest component in each observed redshift;
- the gravitational redshifts are quantized, according to the Karlsson sequence.

The reality of these assumptions will be tested with the results and the relations obtained. Even one failure of the above assumptions will lead to inconsistent results. Radii of local quasars could be determined from:

$$\log(r_q/r_o) = \frac{1}{2} \cdot \log(L_q/L_o) + 2 \log(T_o/T_q) \quad (4)$$

In eq (4), r, L, and T are the radius, luminosity, and the temperature, respectively. Symbols “q” and “o” stay for quasar and for the Sun, respectively. Implementation of this relation needs the assumption of a thermal outer layer. There is an additional question: do large redshifts introduce errors in the radii determination? Since a direct answer to this problem seems difficult, the same strategy will be applied again. Even one false assumption will lead to inconsistent results.

We could further determine the ratio r_{gr}/r_q (r_{gr} is the gravitational radius) from:

$$(1 + z_{gr}) = (1 - r_{gr}/r_q)^{-1/2} \quad (5)$$

Substituting respective z_{gr} for each quasar and the r_q , we can get the quasar gravitational radius r_{gr} . The gravitational radius and the quasar mass m_q are related by:

$$r_{gr} = 2Gm_q/c^2 \quad (6)$$

with G and c being the gravitational constant and the velocity of light. It is now possible to determine also the quasar density ρ_q . Redshifts, magnitudes and colours for quasars are taken from Veron-Cetty and Veron, 13th ed. [61]. In Table 2, the physical characteristics of the 116 sample quasars are listed (not included in [59]).

For all quasars with unknown B – V, quasar radii are determined from the absolute mag – radius relation [18]:

$$M_q = 48.099 - 4.318 \cdot \log r_q$$

In [18], the following density relation was established:

$$\rho_q = 3/(8\pi) \cdot c^2/G \cdot 1/r_q^2 \cdot \{1 - 1/(1 + z_{gr})^2\} \quad (7)$$

This is the relation between quasar density and its gravitational redshift. For local quasars, the gravitational redshift seems to be the main component of the observed redshift and it should be possible to compare computed density data for local quasars with eq (7). This comparison should provide also the test for validity of the assumptions made above. As eq (7) contains also the inverse square of quasar radius, it is

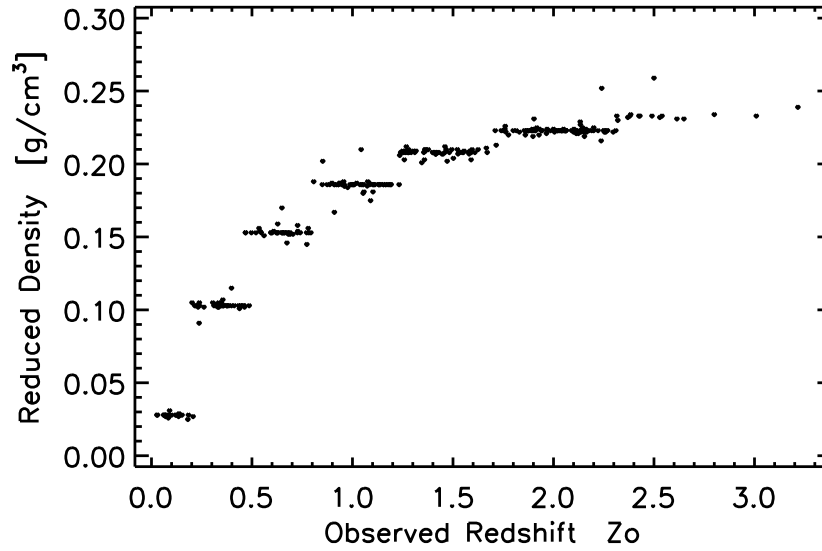


Fig. (1). "Reduced density- observed redshift" diagram for the sample of 341 quasars. All densities are reduced to a radius of $8 \cdot 10^{13}$ cm.

necessary to first reduce all density data to some radius of choice, e.g. $r_q = 8 \cdot 10^{13}$ cm, in order to avoid the dependence on radius. This radius is arbitrary and already used in [18, 59]. The reduced density is:

$$\rho \sim = (r_q / 8 \cdot 10^{13})^2 \cdot \rho_q \quad (8)$$

With this substitution, eq (7) becomes:

$$\rho \sim = 3/(8\pi) \cdot c^2/G \cdot 1/(8 \cdot 10^{13})^2 \cdot \{1 - 1/(1 + z_{gr})^2\} \quad (9)$$

This is the same as eq (7) but with a fixed radius $r_q = 8 \cdot 10^{13}$ cm.

The choice of fixed radius is not essential for conclusions that follow. Data for the reduced densities are also listed in Table 2 and shown in Fig. (1) (altogether 341 QSOs). Densities are plotted versus the observed z_o redshifts, although eq (9) should actually be plotted with the gravitational redshifts only. This causes a spread of the data in the z direction, which is tolerable for small cosmological redshifts (nearly parent galaxies). The reduced densities $\rho \sim$, corresponding to respective gravitational redshifts of the Karlsson sequence can be reckoned from eq (9):

Karlsson sequence of z_{gr} : 0.06, 0.30, 0.60, 0.96, 1.41, 1.96, 2.64, .. Reduced densities $\rho \sim$ [g/cm³]: 0.028; 0.103; 0.153; 0.186; 0.208; 0.223; 0.233;

From Fig. (1), the observational data for all the 341 QSOs fit well to the eq (9). The agreement of observational data with the eq (9) could only be understood as confirmation of this procedure, including all the assumptions made above. The possibility of a coincidence seems very unlikely. More arguments against coincidence will be given below. Possible errors in Fig. (1), contributing to the scatter in the density, could be due to observational errors, variability of quasars, determination of radii from red-shifted spectra, or a projection of a distant (not local) quasar. We should also keep in mind that a part of the galaxy redshift could also have a non-cosmological origin, which could also contribute to errors. The scatter of data in the z -direction is simply due to the use of observed z_o redshifts, instead of the gravitational z_{gr} redshifts, as mentioned above.

If the relation on Fig (1) is real, as it seems, what could be the physics behind it? It is obvious that the SQM could not provide a clue. As pointed out in [18, 59] the relation on Fig. (1) could present evolution of quasars with decreasing density and a corresponding drop of the redshift (actually, only the gravitational component drops because of density). It looks, however, not to be a smooth, continuous transition, but a series of jumps to lower densities and corresponding redshift jumps to next lower value of the Karlsson sequence. This scenario has already been suggested by Arp [45]. Decreasing density could mean disintegration of matter. Such a possibility may seem exotic but I shall seriously take it into consideration and check possible consequences. Additional arguments of the "disintegration scenario" will be discussed below.

The density curve goes apparently to an asymptotic limit with increasing gravitational redshift [18]. As a consequence, at large redshifts only a small drop in density causes a large decrease in the gravitational redshift and respective drop in the observational redshift too. This could account for the decreasing number of QSOs with redshifts $z_o > 3$ and for the absence of very large redshifts.

3. THE LINEAR DENSITY EQUATION.

From eq (5) it follows:

$$r_{gr}/r_q = \{1 - 1/(1 + z_{gr})^2\}$$

Substituting r_{gr}/r_q in eq (7), we get:

$$\rho_q = 3/(8\pi) \cdot c^2/G \cdot 1/r_q^2 \cdot r_{gr}/r_q \quad (10)$$

In eq (10), the quasar density also depends on the inverse square of radius. The same strategy could be applied also in this case by substituting $\rho \sim$ from eq (8) to reduce the density to $r_q = 8 \cdot 10^{13}$ cm. We get the simple linear density equation:

$$\rho \sim = 3/(8\pi) \cdot c^2/G \cdot 1/(8 \cdot 10^{13})^2 \cdot r_{gr}/r_q \quad (11)$$

of the type: $y = a + bx$, where $\mathbf{x} = \mathbf{r}_{gr}/\mathbf{r}_q$, $a = 0$ and b depends on the choice of radius in eq (8). For the following consideration this choice is not essential and I will keep the choice

Table 2. Physical Characteristics of 116 Sample Quasars. Columns are: 1 – ID of Quasar, According to Table 1; 2 – Observed Redshift; 3 – Gravitational Redshift; 4 - Doppler shift; 5 – Absolute Magnitude; 6 – $\log r_q$ [cm]; 7 – $\log L_q$ [erg/s]; 8 – $\log m_q$ [g]; 9 – Density ρ_q [g/cm³]; 10 – Reduced Density [g/cm³] to Radius of $8 \cdot 10^{13}$ cm; 11 – Ratio r_g/r_q ; 12 – Quasar Mass in Units of 10^6 Solar Masses

1	2	3	4	5	6	7	8	9	10	11	12
	NGC 007										
Q1	2.062	1.96	0.029	-12.17	13.958	40.344	41.734	0.173	0.223	0.89	270.9
Q2	2.041	1.96	0.022	-10.96	13.677	39.860	41.454	0.630	0.223	0.89	142.1
Q3	1.591	1.41	0.070	-11.47	13.796	40.064	41.542	0.342	0.208	0.83	174.3
	NGC 470										
Q1	1.533	1.41	0.043	-14.50	14.497	41.276	42.244	0.014	0.208	0.83	877
Q2	1.875	1.96	-0.036	-13.20	14.196	40.756	41.972	0.058	0.223	0.89	469.2
	NGC 520										
Q1	1.670	1.41	0.099	-13.62	14.293	40.924	42.040	0.035	0.208	0.83	548.5
Q2	0.311	0.30	0.001	-13.32	14.224	40.804	41.664	0.023	0.103	0.41	230.6
Q3	2.000	1.96	0.005	-12.02	13.923	40.284	41.699	0.203	0.223	0.89	250.1
Q4	1.609	1.41	0.074	-12.42	14.016	40.444	41.762	0.124	0.208	0.83	289.3
Q5	2.090	1.96	0.035	-12.92	14.131	40.644	41.908	0.078	0.223	0.89	404.2
Q6	1.902	1.96	-0.027	-13.02	14.154	40.684	41.931	0.070	0.223	0.89	426.3
	NGC 936										
Q1	2.042	1.96	0.023	-12.96	14.141	40.660	41.917	0.075	0.223	0.89	412.9
Q2	2.176	1.96	0.068	-12.72	14.147	40.564	41.923	0.072	0.223	0.89	419.1
Q3	1.130	0.96	0.081	-12.43	14.023	40.448	41.721	0.107	0.186	0.74	263.2
	NGC 2683										
Q1	1.252	1.41	-0.067	-10.94	13.735	39.852	41.482	0.452	0.208	0.83	151.5
Q2	1.262	1.41	-0.063	-10.33	13.827	39.608	41.574	0.296	0.208	0.83	187.3
Q3	0.065	0.06	0.004	-11.38	13.775	40.028	40.645	0.050	0.028	0.11	22.1
Q4	0.621	0.60	0.012	-12.19	13.792	40.352	41.406	0.255	0.153	0.61	127.4
	NGC 2841										
Q1	0.120	0.06	0.055	-12.32	13.992	40.404	40.863	0.018	0.028	0.11	36.4
Q2	2.028	1.96	0.021	-11.74	13.771	40.172	41.547	0.409	0.223	0.89	176.3
	NGC 2859										
Q1	0.230	0.30	-0.059	-13.29	14.301	40.792	41.741	0.016	0.103	0.41	275.5
Q2	2.250	1.96	0.092	-12.33	13.995	40.408	41.771	0.146	0.223	0.89	295.1
Q3	1.460	1.41	0.015	-11.73	13.856	40.168	41.603	0.259	0.208	0.83	200.2
Q6	0.027	0.06	-0.037	-13.53	14.273	40.888	41.143	0.005	0.028	0.11	69.5

Table 2. contd...

1	2	3	4	5	6	7	8	9	10	11	12
	NGC 2916										
Q1	1.546	1.41	0.044	-13.81	14.346	41.000	42.093	0.027	0.208	0.83	619.0
Q2	0.238	0.30	-0.059	-13.84	14.344	41.012	41.784	0.013	0.103	0.41	304.3
Q3	0.793	0.60	0.107	-14.04	14.391	41.092	42.004	0.016	0.153	0.61	505.0
Q4	1.868	1.96	-0.043	-13.69	14.066	40.952	41.842	0.105	0.223	0.89	347.6
Q5	1.279	1.41	-0.066	-13.95	14.451	41.056	42.198	0.017	0.208	0.83	788.8
	NGC 3184										
Q1	0.675	0.60	0.045	-12.11	13.750	40.320	41.364	0.310	0.153	0.61	115.6
Q2	0.920	0.96	-0.022	-11.13	13.810	39.928	41.508	0.286	0.186	0.74	161.1
Q3	0.152	0.06	0.085	-12.64	14.066	40.532	40.937	0.013	0.028	0.11	43.2
	NGC 3384										
Q1	0.442	0.30	0.077	-10.94	13.588	39.852	41.028	0.439	0.103	0.41	53.3
Q2	1.280	1.41	-0.081	-10.98	13.770	39.868	41.517	0.384	0.208	0.83	164.6
Q4	1.107	0.96	0.044	-11.19	13.710	39.952	41.408	0.453	0.186	0.74	127.9
Q5	1.192	0.96	0.086	-10.25	13.513	39.576	41.211	1.122	0.186	0.74	81.3
Q8	1.134	0.96	0.057	-11.69	14.015	40.152	41.713	0.111	0.186	0.74	258.1
Q13	0.497	0.60	-0.092	-10.68	13.797	39.748	41.411	0.250	0.153	0.61	128.9
Q14	0.520	0.60	-0.078	-10.31	13.485	39.600	41.099	1.051	0.153	0.61	62.8
Q15	1.131	0.96	0.056	-10.49	13.767	39.672	41.465	0.348	0.186	0.74	145.8
	NGC 3516										
Q1	2.100	1.96	0.038	-14.45	14.486	41.256	42.262	0.015	0.222	0.89	914.0
Q2	1.399	1.41	-0.013	-12.95	14.138	40.656	41.885	0.071	0.208	0.83	383.8
Q3	0.930	0.96	-0.024	-12.95	14.138	40.656	41.836	0.063	0.186	0.74	342.9
Q4	0.690	0.60	0.047	-13.85	14.347	41.016	41.960	0.020	0.153	0.61	456.5
Q5	0.328	0.30	0.012	-12.75	14.092	40.576	41.532	0.043	0.103	0.41	170.1
Q6	1.710	1.96	-0.093	-14.35	14.462	41.216	42.239	0.017	0.223	0.89	866.5
	NGC 3842										
Q1	0.335	0.30	0.005	-16.21	14.893	41.960	42.333	0.001	0.102	0.41	1076.5
Q2	0.946	0.96	-0.028	-15.63	14.586	41.728	42.284	0.008	0.186	0.74	960.5
Q3	2.200	1.96	0.059	-14.53	14.378	41.288	42.154	0.025	0.223	0.89	713.5
	NGC 6212										
Q1	1.864	1.96	-0.060	-15.68	14.596	41.748	42.372	0.0092	0.223	0.89	1177.0
Q2	2.010	1.96	-0.013	-14.20	14.206	41.156	41.982	0.0553	0.223	0.89	479.6

Table 2. contd...

1	2	3	4	5	6	7	8	9	10	11	12
Q3	1.898	1.96	-0.049	-15.87	14.835	41.824	42.611	0.003	0.219	0.89	2043.5
Q4	0.461	0.30	0.091	-18.07	15.138	42.704	42.578	0.0004	0.103	0.41	1891.5
Q5	0.143	0.06	0.047	-17.12	15.085	42.324	41.955	0.0001	0.028	0.11	451.3
Q6	0.030	0.06	-0.057	-17.70	15.238	42.556	42.109	0.0001	0.028	0.11	642.0
Q7	1.965	1.96	-0.027	-16.30	14.914	41.996	42.690	0.0021	0.221	0.89	2451.0
Q8	1.183	0.96	0.081	-15.10	14.443	41.516	42.141	0.016	0.186	0.74	692.0
Q9	1.666	1.41	0.074	-16.13	14.875	41.928	42.622	0.0024	0.211	0.83	2092.0
Q10	2.253	1.96	0.067	-16.42	14.684	42.044	42.460	0.0061	0.222	0.89	1441.5
Q11	1.625	1.41	0.058	-16.90	14.780	42.236	42.527	0.0037	0.210	0.83	1680.7
Q12	2.614	2.64	-0.036	-16.41	14.648	42.040	42.442	0.0075	0.231	0.92	1384.9
Q13	0.540	0.60	-0.066	-15.67	14.522	41.744	42.136	0.009	0.154	0.61	683.5
Q14	1.005	0.96	-0.007	-17.45	14.950	42.456	42.648	0.002	0.186	0.74	2221.0
Q15	0.625	0.60	-0.014	-14.99	14.252	41.472	41.865	0.031	0.153	0.61	366.8
Q16	2.529	2.64	-0.059	-15.18	14.610	41.548	42.405	0.009	0.232	0.92	1271.0
Q17	1.860	1.96	-0.062	-16.65	14.923	42.136	42.700	0.002	0.220	0.89	2504.5
Q18	1.580	1.41	0.039	-14.65	14.495	41.336	42.242	0.0136	0.207	0.83	872.5
Q19	1.595	1.41	0.045	-15.88	14.661	41.828	42.408	0.0064	0.210	0.83	1278.0
Q20	1.466	1.41	-0.007	-16.03	14.780	41.888	42.527	0.0037	0.210	0.83	1683.5
Q21	1.414	1.41	-0.027	-15.50	14.665	41.676	42.412	0.0062	0.207	0.83	1291.0
Q22	2.384	2.64	-0.098	-16.23	14.681	41.968	42.476	0.0065	0.234	0.92	1496.0
Q23	0.595	0.60	-0.032	-18.91	15.217	43.040	42.831	0.0004	0.153	0.61	3387.5
Q24	1.360	1.41	-0.049	-17.26	14.937	42.380	42.684	0.0018	0.210	0.83	2413.0
Q25	2.000	1.96	-0.016	-15.49	14.498	41.672	42.274	0.0144	0.223	0.89	939.5
Q26	2.260	1.96	0.069	-15.48	14.680	41.668	42.456	0.0062	0.222	0.89	1428.5
Q27	2.000	1.96	-0.016	-14.68	14.434	41.348	42.210	0.0194	0.223	0.89	811.0
Q28	0.443	0.30	0.078	-16.20	14.362	41.956	41.802	0.0124	0.103	0.41	317.2
Q29	0.704	0.60	0.034	-17.18	14.749	42.348	42.362	0.0031	0.152	0.61	1151.5
Q30	1.083	0.96	0.032	-16.44	14.773	42.052	42.471	0.0034	0.187	0.74	1478.0
Q31	2.113	1.96	0.021	-16.19	14.698	41.952	42.474	0.0057	0.221	0.89	1488.5
Q32	0.594	0.60	-0.033	-16.00	14.426	41.876	42.040	0.014	0.153	0.61	547.5
Q33	1.358	1.41	-0.050	-16.95	14.983	42.256	42.730	0.0014	0.203	0.83	2687.0
Q34	0.434	0.30	0.071	-16.11	14.599	41.920	42.039	0.004	0.103	0.41	546.5
Q35	1.377	1.41	-0.042	-16.05	14.747	41.896	42.494	0.0043	0.210	0.83	1560.5
Q36	0.608	0.60	-0.024	-16.37	14.438	42.024	42.052	0.013	0.154	0.61	563.0
Q37	1.268	1.41	-0.086	-16.19	14.964	41.952	42.711	0.0016	0.212	0.83	2570.0
Q39	1.451	1.41	-0.012	-16.46	14.669	42.060	42.416	0.006	0.207	0.83	1302.0
Q40	1.877	1.96	-0.056	-16.01	14.500	41.880	42.276	0.0143	0.223	0.89	943.5

Table 2. contd...

1	2	3	4	5	6	7	8	9	10	11	12
Q41	2.145	1.96	0.031	-15.89	14.743	41.832	42.519	0.0047	0.225	0.89	1653.0
Q42	0.100	0.06	0.008	-17.90	15.040	42.636	41.910	0.0002	0.028	0.11	406.4
	Mark 231										
Q1	0.320	0.30	-0.025	-18.15	15.176	42.736	42.616	0.0003	0.103	0.41	2067.0
Q2	0.124	0.06	0.018	-19.06	15.553	43.100	42.424	1x10 ⁻⁵	0.028	0.11	1326.0
Q3	1.272	1.41	-0.095	-15.39	14.763	41.632	42.510	0.0040	0.208	0.83	1617.5
Q4	1.232	0.96	0.093	-16.50	14.865	42.076	42.563	0.0022	0.186	0.74	1827.5
Q5	1.190	0.96	0.072	-16.75	14.835	42.176	42.533	0.0026	0.186	0.74	1705.0
Q6	0.330	0.30	-0.018	-17.43	14.874	42.448	42.314	0.0012	0.102	0.41	1030.5
Q7	0.072	0.06	-0.029	-18.91	15.293	43.040	42.163	5x10 ⁻⁵	0.028	0.11	727.5
	Mark 273										
Q1	0.207	0.06	0.098	-17.65	15.505	42.536	42.375	2x10 ⁻⁵	0.027	0.11	1187.0
Q2	0.941	0.96	-0.045	-18.44	15.173	42.852	42.871	0.0005	0.187	0.74	3712.5
Q3	0.458	0.30	0.082	-15.31	14.685	41.600	42.125	0.0028	0.103	0.41	666.0
Q4	1.166	0.96	0.066	-17.33	15.059	42.408	42.757	0.0009	0.186	0.74	2860.0
Q5	0.486	0.30	0.102	-16.63	14.594	42.128	42.034	0.0043	0.103	0.41	540.5
Q6	0.377	0.30	0.022	-16.66	14.926	42.140	42.365	0.0009	0.103	0.41	1159.5
	AM 2230-284										
Q1	2.141	1.96	-0.003	-17.14	15.109	42.332	42.885	0.0009	0.223	0.89	3835.5
Q2	2.152	1.96	0.001	-16.40	14.937	42.036	42.713	0.0019	0.222	0.89	2585.0
Q3	2.165	1.96	0.005	-17.56	15.206	42.500	42.982	0.0006	0.222	0.89	4798.5
Q4	2.161	1.96	0.004	-16.92	15.058	42.244	42.834	0.0011	0.224	0.89	3411.0
Q5	2.155	1.96	0.002	-17.14	15.109	42.332	42.885	0.0009	0.222	0.89	3835.5
Q6	2.134	1.96	-0.005	-16.58	14.979	42.108	42.755	0.0016	0.227	0.89	2845.5
Q7	2.133	1.96	-0.005	-16.59	14.981	42.112	42.758	0.0016	0.229	0.89	2860.5
Q8	2.154	1.96	0.001	-16.74	15.016	42.172	42.792	0.0013	0.219	0.89	3099.0
Q10	2.155	1.96	0.002	-16.31	14.916	42.000	42.693	0.0021	0.223	0.89	2464.0
Q11	2.136	1.96	-0.004	-16.68	15.002	42.148	42.778	0.0014	0.222	0.89	3001.5
Q12	2.168	1.96	0.006	-16.24	14.900	41.972	42.676	0.0023	0.223	0.89	2373.5
Q13	2.139	1.96	-0.003	-17.07	15.092	42.304	42.869	0.0009	0.223	0.89	3695.0
Q14	2.137	1.96	-0.004	-16.71	15.009	42.160	42.785	0.0014	0.223	0.89	3049.8

in eq (8) and in eq (11). Then in the [cm, g, s] system, b = 0.251549 in eq (11). We therefore get:

$$\rho \sim 0.251549 \cdot r_{gr} / r_q \tag{12}$$

The sample of 341 QSOs (Table 2, this study, and [59]) are plotted in Fig. (2). The straight line is obvious, and the coefficients are: a = 0.0002 and b = 0.251. Let me now turn back to the question: could this be a coincidence? Although

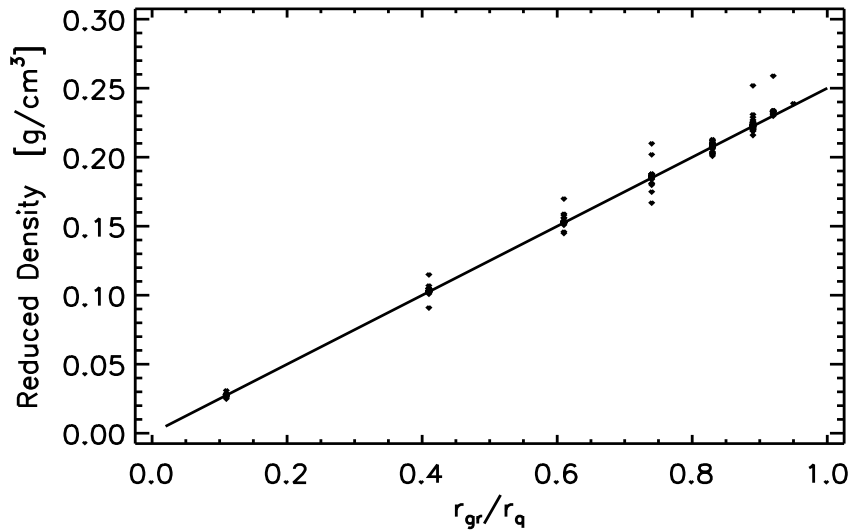


Fig. (2). The linear relation of quasar reduced density with r_{gr}/r_q for the sample of 341 QSOs. The mean line equation is: $\rho \sim 0.0002 + 0.251 \cdot r_{gr}/r_q$ (see text).

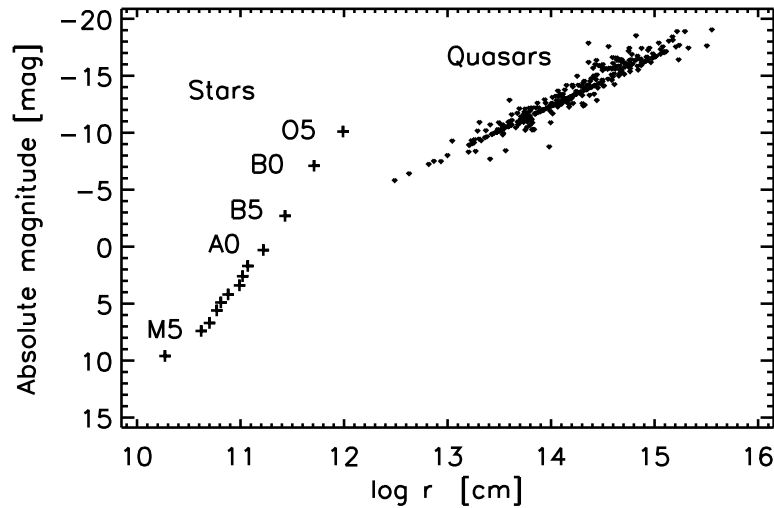


Fig. (3). The relation “absolute magnitude – radius” for 341 sample quasars (dots). The same relation is shown also for stars (crosses), as mean values for O5, B0, ..., M5.

very unlikely, both relations, on Fig. (1) and on Fig. (2) considered separately could be due to a coincidence. However, there is now an additional argument. How is it possible that these two “coincidences” are related? Their relation is obvious. The eq (12) follows from eq (7). Coincidences can not be related, or else they are not coincidences. In the following, additional arguments will be presented for the credibility of the procedure. Reducing densities to a different radius will produce a different slope coefficient in eq (12) but this is not essential for the results and the conclusions. The slight deviation of coefficients “a” and “b” from the respective theoretical values in eq (12) are likely to be due to observational uncertainties. As will be shown, the linear density equation (12) could be applied also to other structures.

4. SOME RELATIONS FOR QUASARS

In Fig. (3), the absolute magnitude is plotted versus radius for the sample of 341 QSOs. The sequence of stars is also shown as mean values for O5, B0, B5, A0,, M5.

There is a good agreement with the respective relation in [18, 59]. Therefore, by increasing the QSOs sample this relation is confirmed.

In Fig. (4), the absolute magnitude is plotted against the mass for 341 sample QSOs. Shown is also the sequence of stars. There is a good agreement with the respective relation from [18, 59].

The “mass-radius” relation is shown in Fig. (5) for the sample of 341 QSOs. The sequence of stars is also shown. The agreement with [18, 59] is good. It has already been pointed out in [18, 59] that this “mass-radius” relation implies that fainter quasars have larger gravitational redshifts (leading to larger observed redshifts), which has been discussed already by Greenstein and Schmidt [6]. The mean “mass-radius” relation for 341 sample QSOs is:

$$\log m_q = 28.67 + 0.93 \log r_q \tag{13}$$

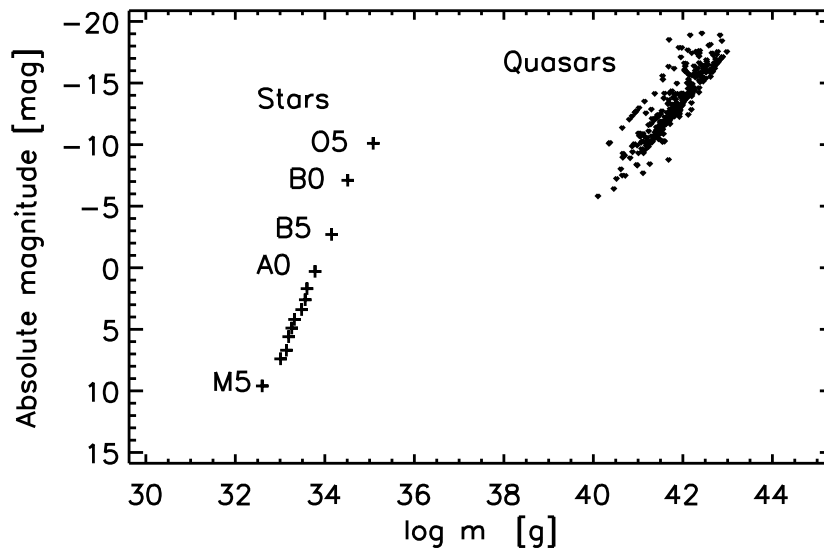


Fig. (4). The relation “absolute magnitude – mass” for 341 sample quasars (dots). The same relation is shown also for stars (crosses), as mean values for O5, B0, B5, ..., M5.

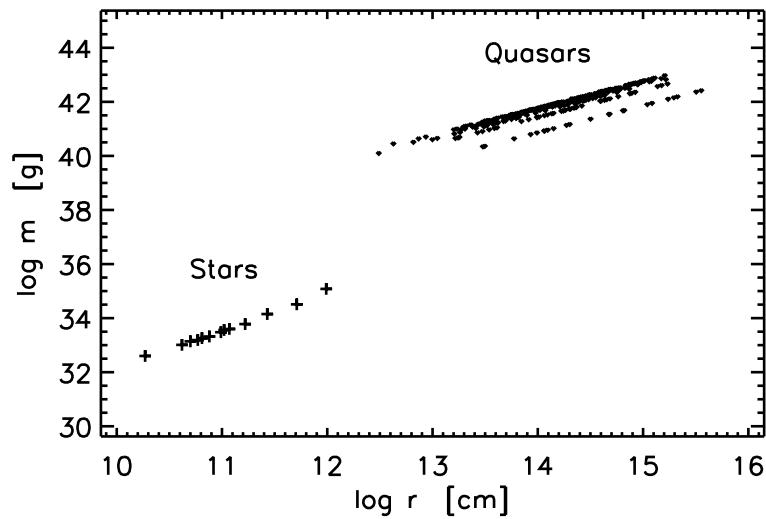


Fig. (5). The relation “mass – radius” for 341 sample quasars (dots). The same relation is shown also for stars (crosses), as mean values for O5, B0, B5, ..., M5.

The “mass-luminosity” relation is shown in Fig. (6) for the sample of 341 QSOs.

The stellar sequence is also shown. The mean “mass-luminosity” relation for 341 QSOs is:

$$\log L_q = -27.49 + 1.63 \cdot \log m_q \tag{14}$$

in agreement with [18,59]. The physics behind these relations is not yet clear.

5. EVIDENCE OF EVOLUTION OF QUASARS.

Possible evolutionary scenario has already been mentioned by the discussion of Fig. (1). Quasars seem to evolve with decreasing redshifts because of decreasing density. From that scenario, other relations could also be expected and they will be looked for in this section. In the first place, evolutionary effects could be searched for by comparing groups of quasars at different distances. This is shown in Fig. (7) and Fig. (8), where plots of quasar absolute magnitude

(Fig. (7)) and quasar mass (Fig. (8)) versus respective redshift of parent galaxy are presented. Both the quasar absolute magnitude and the quasar mass increase with the cosmological redshift, i.e. with distance ($z_{gal} = z_c$).

As pointed out in [18, 59], in order to study evolutionary effects on luminosity with decreasing gravitational redshift, it was necessary to sample QSOs in different groups (see Fig. (3) in [59]). It is now apparent that this sampling corresponds to the respective redshift of parent galaxy, i.e. to the cosmological quasar redshift. As apparent from Fig. (7) and Fig. (8), at earlier stages of the Universe, at least to a distance, corresponding to $z_{gal} = 0.064$, the quasars seem to have larger masses and larger luminosities. The reason for that remains unclear. Especially strong is the dependence of luminosity and mass of QSOs in the parts of the diagrams below cosmological redshift of about 0.003. Apparently, if a study of evolutionary effects of mass and luminosity of quasars due to z_{gr} is to be correct, the dependence on distance

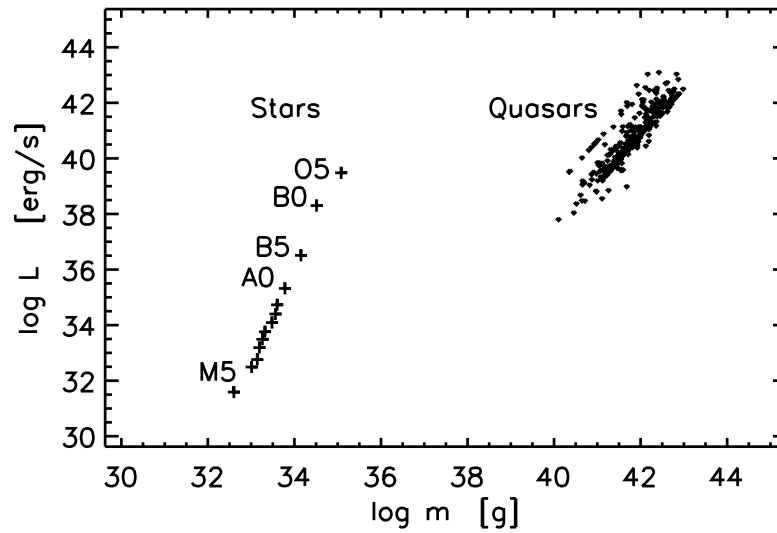


Fig. (6). The “mass-luminosity” relation for 341 sample quasars (dots). The same relation is shown also for stars (crosses), as mean values for O5, B0, B5, ..., M5.

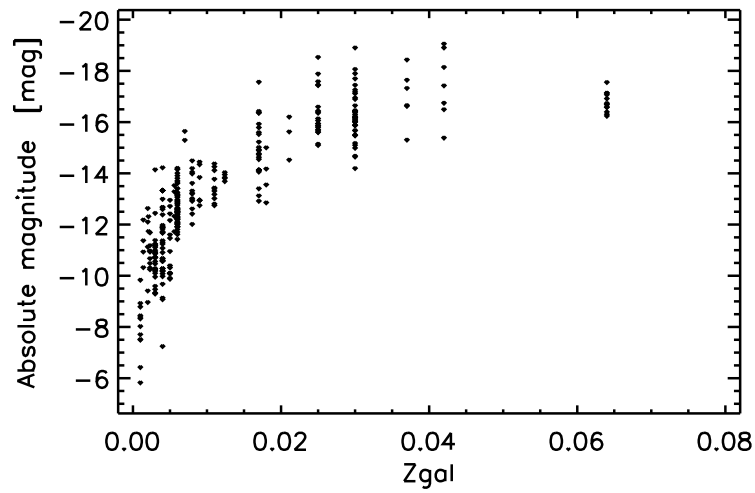


Fig. (7). Dependence of quasar absolute magnitude on distance for 341 sample QSOs. Note the increasing “mean” luminosity to about $z_{gal} = 0.025$.

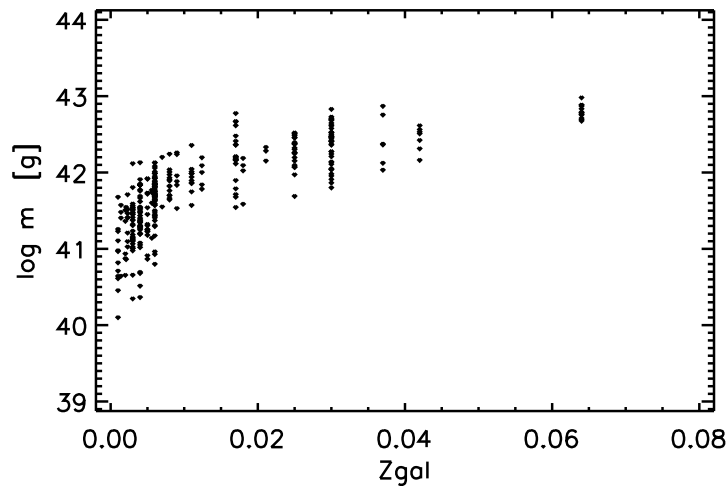


Fig. (8). Dependence of quasar mass on distance for 341 sample QSOs. Note the increasing “mean” mass to about $z_{gal} = 0.025$.

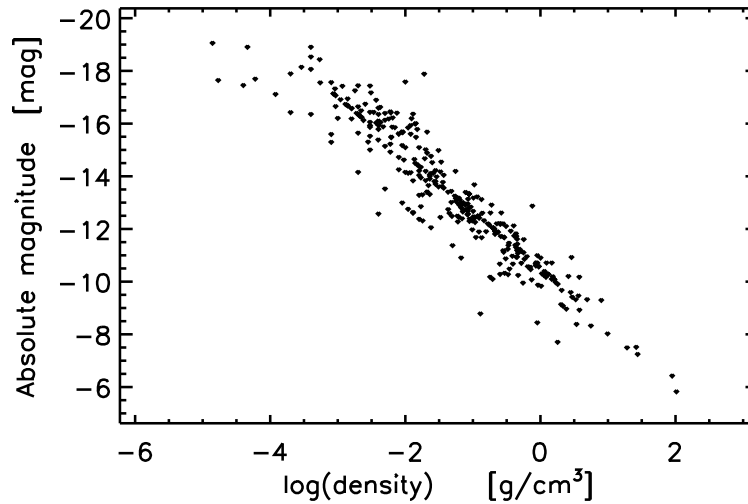


Fig. (9). Relation “absolute magnitude – density” for 341 sample quasars.

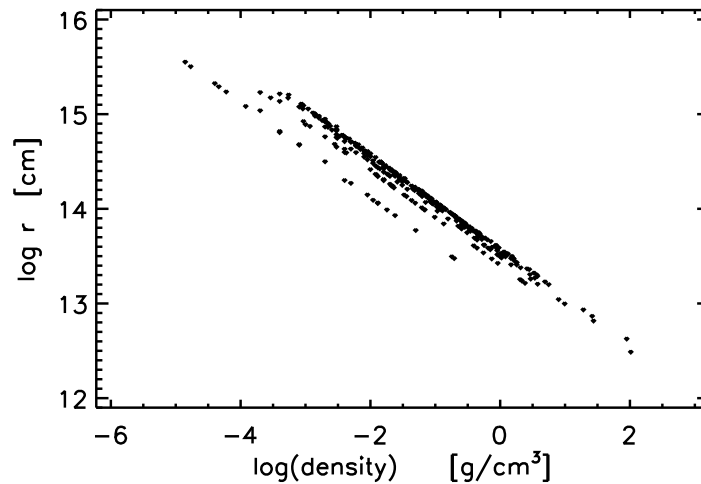


Fig. (10). Relation “radius – density” for 341 sample quasars.

should be taken into account. Evolution with decreasing density and preserved mass of quasar would imply possible relation between quasar density and radius. In [18, 59], an evolutionary increase of quasar luminosity and radius was suggested. Looking for further evidence of evolutionary effects, in Fig. (9) is plotted the quasar absolute magnitude versus quasar density. From Fig. (9), the apparent relation is in the sense that larger luminosities correspond to lower density (the presumed direction of evolution).

From Fig. (9), in direction of increasing density, quasars get less luminous. This relation prompts further tantalizing questions. Is it possible to extend the relation to even larger densities? If yes, could this relation have a bearing on the much discussed problem of the hidden (dark) mass? Is it possible that the “dark” masses could be faint because of high density?

In Fig. (10), quasar radius is plotted versus quasar density. The obvious trend of increasing radius by decreasing density is consistent with the disintegration hypothesis.

Quasar absolute magnitude (Fig. 11) and quasar radius (Fig. 12) are plotted versus quasar redshift z_0 , as a check for

consistency. The presumed direction of evolution is decreasing redshift. On these diagrams, as well as on Fig. (13), quasars with cosmological redshift less than 0.003 are not included, in order to partly avoid respective dependence on distance. The large scatter on these plots is possibly due to the still remaining effects of distance dependence. Yet, the absolute magnitude and the radius seem to be possibly increasing with decreasing redshift, according to the evolutionary scenario.

An interesting question is, are there any evolutionary effects observed in the quasar masses? According to the Arp’s scenario [45], quasars develop into galaxies. Building a stellar population around a quasar requires (if the total mass is preserved) that at some stage of the evolution quasars have to start losing mass. Is there any evidence of this process? In Fig. (13) quasar mass is plotted versus the redshift. The interpretation of this diagram is not straight. There could be a mass drop at the late stages of evolution, for $z_0 < 0.60$ but this matter needs further study.

In Fig. (14), a plot of the quasar density versus mass is presented. The apparent trend confirms respective results from [18, 59]. Larger masses correspond to smaller densities.

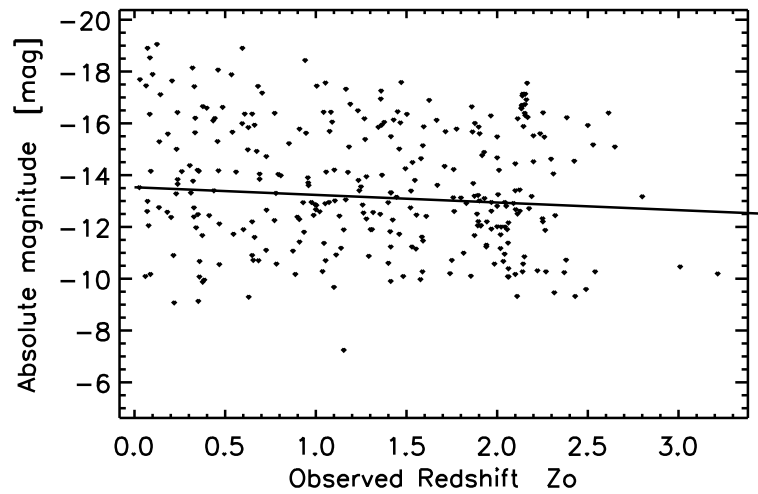


Fig. (11). Plot of quasar absolute magnitudes versus observed redshift for the sample quasars with $z_{\text{gal}} > 0.003$ ($z_{\text{gal}} = z_c$, see text).

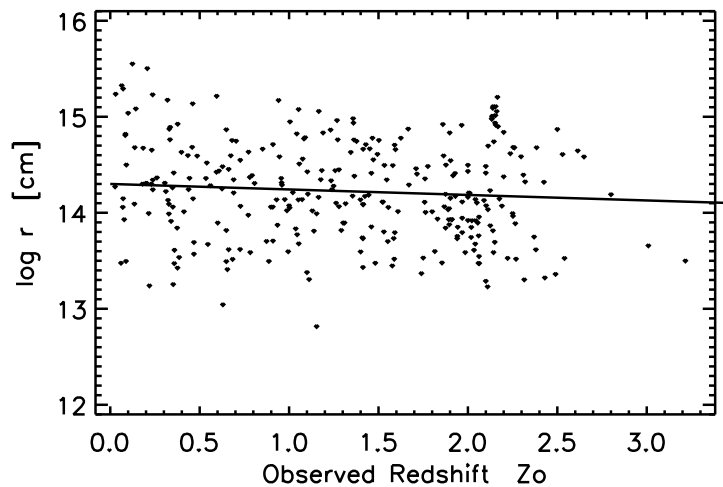


Fig. (12). Plot of quasar radius versus observed redshift for the sample quasars with $z_{\text{gal}} > 0.003$ ($z_{\text{gal}} = z_c$, see text).

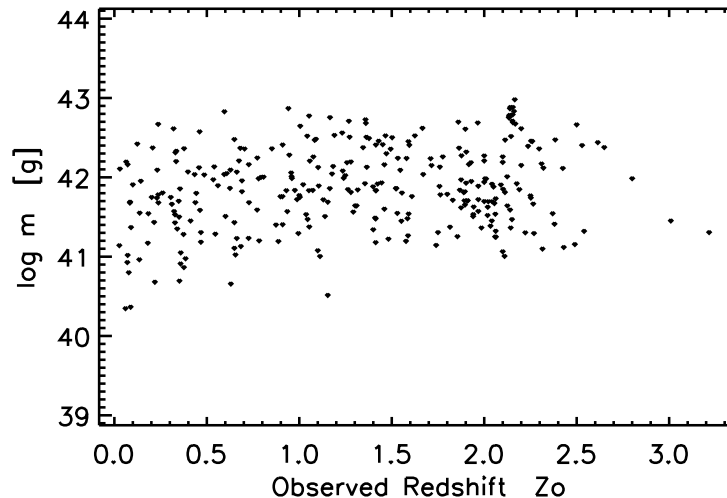


Fig. (13). Plot of quasar mass versus observed redshift for quasars with $z_{\text{gal}} > 0.003$.

If the presumed direction of evolution is towards decreasing densities, the relation on Fig. (14) shows that quasars with larger masses evolve more rapidly.

The concept of evolution due to disintegration of some mysterious dense matter is not a new one. It has been intro-

duced first by Victor Ambartsumian about 60 y ago [87]. It now appears that this concept gets new impetus. The evidence presented in this section seems to support possible consequences of the evolutionary scenario with decreasing density.

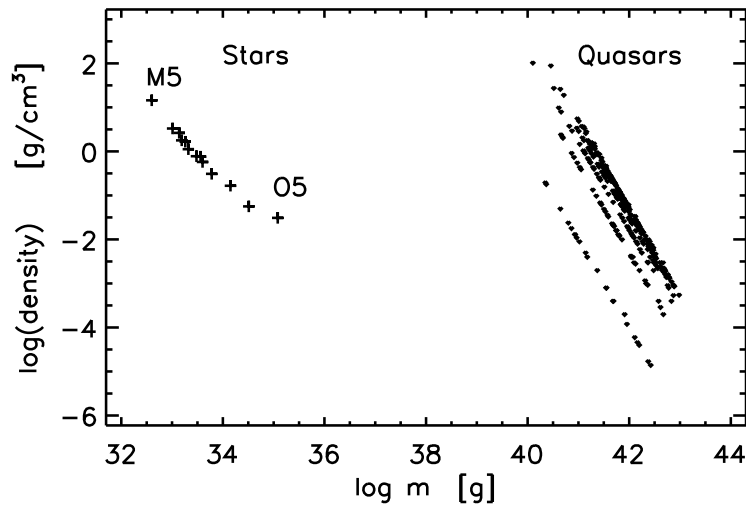


Fig. (14). Relation “mass – density” for the sample of 341 quasars (dots). The same relation is shown for stars (crosses), as mean values for O5, B0, B5, ..., M5.

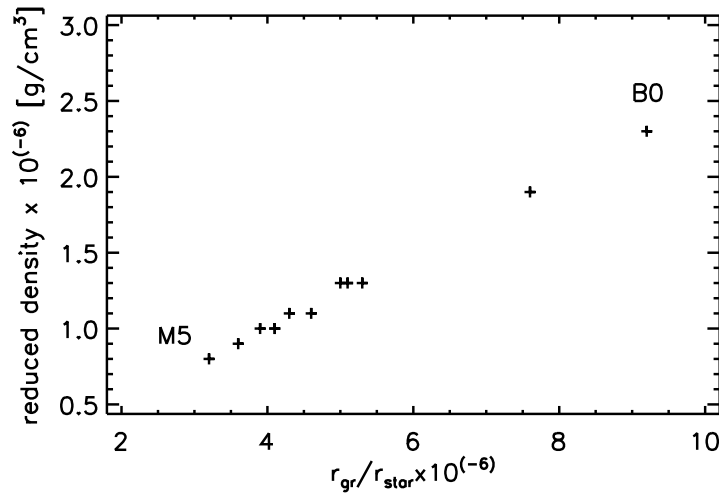


Fig. (15). The linear relation of stellar reduced density (to a radius of $8 \cdot 10^{13}$ cm). with the stellar r_{gr}/r_{star} . The sequence is: B0, B5, A0, F0, A5, F5, G5, G0, K0, M0, M5. The linear equation is: $\rho \sim -2 \cdot 10^{-9} + 0.2505 \cdot r_{gr}/r_{star}$.

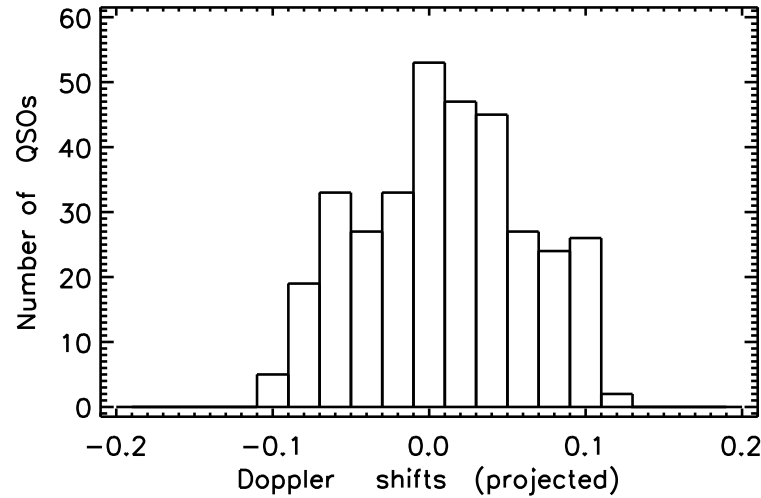
6. IS THERE A QUASAR-STELLAR CONNECTION?

In the previous sections, on Figs. (3-6), and on Fig. (14) the sequence of stars along with quasars were shown. There is a striking similarity when stars and quasars are compared on these figures, although respective relations for stars and quasars are not identical. But what if there would be a relation, identical for quasars and stars? On Fig. (15), the reduced stellar densities (to the same radius of $8 \cdot 10^{13}$ cm) are plotted versus the ratio r_{gr}/r_{star} . This plot corresponds to the plot on Fig. (2) for quasars. Surprisingly, the straight line in Fig. (15) corresponds closely to the linear density equation (12), and the coefficients are: $a = -2 \cdot 10^{-9}$, $b = 0.2505$ (correlation coeff is 0.998). Comparing with respective values for quasars, this is probably the same relation. Deviation of the coeff “a” from zero, and deviation of coeff “b” from the theoretical value 0.251549 are probably due to observational uncertainties in the case of stars, as well as for quasars. Several remarks are due about Fig. (15). Mean data were used for spectral classes B0, B5, A0, ..., M5, therefore this result is significant. The O-stars were omitted because of strong

deviation from the relation. On Fig. (15), the sequence of spectral classes follows from upper right (B0) to lower left (M5) but the spectral classes run not in exactly the same order. These are details that are beyond the scope of this study. The primary significance of this result is that probably it is the same linear density relation, eq. (12), which holds for stars and for quasars. As stellar data could not be put in doubt, this result naturally corresponds to the result for quasars above, shown on Fig. (2). This is additional argument in favour of consistency. Besides, there is now tantalizing evidence that quasars and stars are somehow related. Could this link be expected in the process of their origin? This is yet another surprising hint which is worth to pursue further. One could ask also a question, what about the planets? Could they be fitted with the linear density eq (12)? Unfortunately, only the 9 big planets of the Solar system could be used for that presently and the result could not be significant. Yet, the hint also in this case may look promising. With reduced densities (to the same radius of $8 \cdot 10^{13}$ cm) of the 9 big planets, the coefficients in eq (12) are: $a = 7 \cdot 10^{-11}$ and $b = 0.2579$. Is this another tantalizing hint?

Table 3. Summary of Data for the Solution of $\rho \sim a + b \cdot r_{gr}/r$

	Coeff "a"	Coeff "b"	Correlation Coeff	Range of the Reduced Density [g/cm ³] to $r = 8 \cdot 10^{13}$ [cm]
Eq (12)	0	0.251549	1.0	
QSOs	0.0002	0.251	0.998	0.02 - 0.25
Stars B0-M5	$-2 \cdot 10^{-9}$	0.2505	0.998	$0.8 \cdot 10^{-6}$ - $2.3 \cdot 10^{-6}$
9 Planets	$7 \cdot 10^{-11}$	0.258	0.998	$1.1 \cdot 10^{-11}$ - $1 \cdot 10^{-8}$

**Fig. (16).** Distribution of the projected Doppler shifts of the 341 sample quasars.

In Table 3, data for the solution of the linear density eq (12) is summarized for quasars, stars, and planets.

7. THE DOPPLER-VELOCITIES DISTRIBUTION

The distribution of the Doppler shifts of local quasars is yet unknown. It was discussed in [59] with a sample of 225 QSOs. There are several general assumptions, which seem realistic and are expected to be fulfilled:

- Doppler shifts reflect only the projections of ejection velocity along the line of sight. The real ejection velocities could be larger.

- Lower ejection velocities are more likely because of energy considerations. If the sample of QSOs is large enough, a peak in the distribution would therefore be expected around the zero Doppler shift.

- The distribution should have symmetry with respect to the zero velocity, if all directions of ejection have the same probability. There are reports [19], where the ejection of QSOs is noted to proceed along the minor (rotational) axis of the parent galaxy. This effect, if real, could introduce some distortion of the distribution with smaller samples of QSOs. With a large sample of galaxies and ejected quasars, however, these effects should cancel out and the distribution should be symmetric.

- Ejection velocities should be limited.

The distribution of the sample of 341 QSOs (225 from [59] and 116 from Table 2, present study) is shown on Fig. (16).

The distribution on Fig. (16) of projected Doppler shifts seems to correspond (more or less) to the above considerations. The highest projected velocity seems to be slightly over 30 000 km. s⁻¹.

8. DISCUSSION AND CONCLUDING REMARKS.

Discussion about clustering of quasars around low redshift galaxies goes since about 40 years ago. The hypothesis of gravitational reddening makes it possible to get some of the physical characteristics of local quasars and to establish relations between them. These findings seem to be in agreement with the Arp's [45, 88] scenario - local quasars are probably ejected by active galactic nuclei due to yet unknown physical process. All conclusions and considerations here refer to only the sample of 341 QSOs (116 from this study, and 225 QSOs from [59]). Some conclusions seem quite radical. On the other hand, the sample presented is not negligible, and the conclusions are not unfounded. Generally, the results presented here confirm respective results from [18, 59].

Local quasars probably cluster around low redshift active galaxies, because probably being ejected by their respective nucleus. The highest projected velocity of ejection could be about 30 000 km. s⁻¹. The physics of this ejection is yet unknown. Quasars are likely to be single objects, with dimensions close to their respective gravitational radius. A theory of such massive bodies does not yet exist. Their internal structure is yet unknown and our present knowledge seems insufficient to explain how such massive bodies exist. QSOs could evolve with decreasing density and redshifts, which could be due to disintegration of matter of yet unknown ori-

gin and properties. At the beginning, the evolution of quasar-redshifts due to decreasing density is very fast. This could explain the decreasing number of QSOs with $z > 3$. Such quasars could evolve very fast to lower values of redshift. Another consequence to be expected by this evolution scenario is the increase of radius of quasars. The end product of evolution of local quasars could be small mass companion galaxies. Galaxies beget companion galaxies? This scenario should be considered seriously. If confirmed, such a scenario could probably require re-considering the theory of origin of galaxies in general. On the “density-redshift” diagram, there are no quasars below reduced density $\sim 0.02 \text{ g/cm}^3$. Could it be that QSOs have already evolved into galaxies? There could be yet another important implication. If quasars develop into galaxies, it would be possible to expect small gravitational components to exist also in the redshifts of some galaxies, which are still in transition (compact galaxies). Possible presence of gravitational reddening in distant galaxies may require introducing small corrections of the Hubble diagram and the Hubble relation.

It has been discussed in the past that if quasars would be of local origin that would contradict the Big Bang theory. This is not necessarily so. In our starting eq (1), taken from [60], a term of the expanding Universe is included. The expansion of the Universe and the gravitational reddening could be two different sources attributing to the redshifts of extragalactic sources. The problem would be how we could disentangle these two components? For local quasars, the observed redshifts could be decomposed rather easily to the three components - cosmological component, gravitational reddening, and a Doppler shift. Decomposition of these components in the redshifts of distant objects could prove to be much more difficult. It should be stressed, however, that the concept of local quasars does not contradict the cosmological expansion. It actually makes use of the expansion, when it comes to the effects of evolution. The gravitational redshift seems to be the largest component in local quasars and gravitational redshifts seem to be quantized, according to the Karlsson sequence. The negative result of searching for the Karlsson sequence, when using modern surveys does not necessarily mean that this sequence does not exist. The pattern of this sequence could be undetectable in modern surveys because of strong contribution by the two other components in the observed redshift, especially by the cosmological reddening. In the Arp’s scenario [45, 88], the evolution of redshift proceeds in steps, each step corresponding to the next lower value of the Karlsson sequence. Quantized redshifts are, however, not compatible with our present physics and require new concepts. In order to obtain a sequence of specific gravitational redshifts, the gravitational potential of a quasar has to go by the quasar evolution through a sequence of specific (decreasing) values. How this should be possible is a mystery at present. Quasars are mysterious objects in other respects, too. We may need a deeper insight into the subatomic physics of matter to resolve these problems.

The procedure of determination of radii implies that QSOs should have a thermal outer layer, probably heated from below. This is in contradiction with the most popular theory of SQM. Larger gravitational redshifts seem to correspond to fainter quasars. As a result of the evolution, quasars’ dimensions and luminosities seem to increase. Building

stellar population around a quasar requires a mass. Therefore, QSOs should be losing mass in the process of evolution, in order to keep the total mass constant. There may be a hint that quasars’ masses decrease for redshifts less than 0.60. The process of evolution with decreasing density and building stars around a quasar reminds of the old hypothesis, suggested by Victor Ambartsumian. This concept has so far been largely neglected, because it was not possible to develop and to test specific models. In view of the recent developments this idea may get new attention. Some relations, shown in the section 5, appear to be in agreement with possible consequences of evolution due to disintegration: dimensions and luminosities increase with decreasing density. There is another possible hint, following from the “mass-density” relation. Quasars with larger masses could evolve more rapidly. Interesting evidence may come also from the “density - luminosity” relation. If confirmed, it would appear that more dense bodies are less luminous. Could this relation have a bearing on the much discussed problem of the “hidden” (dark) mass in the Universe?

A new finding here is the dependence of masses and luminosities of QSOs on distance. The evidence would appear to be that more distant quasars (to about $z_c = 0.06$) are also more luminous and more massive. This trend is steep to about $z_{gal} = 0.025$ and then seems to remain flat.

According to the disintegration scenario, in a group of quasars at about the same distance and having the same masses, the QSOs with largest redshifts should be most young.

Several relations for local quasars seem to exist, and each of them has similar (but not identical) counterpart relation for stars. For stars these relations are known for many years. Even more surprising is the linear density relation, eq (12). It appears that this equation holds for quasars, as well as for stars. Could it be that we may be dealing with a fundamental link, possibly having its roots in the origin of quasars and stars?

The possibility of having processes of disintegration as an alternative to the gravitational collapse as the origin of galaxies has been largely neglected in the past years. The implication of this alternative is not excluded, however, by the observational evidence for galaxies, and may be, even for stars. This could open enormous new possibilities.

CONFLICT OF INTEREST

The authors confirm that this article content has no conflicts of interest.

ACKNOWLEDGEMENTS

For this work, I used the SIMBAD and the VizieR databases, operated by CDS, Strasburg, France. My thanks are due to Dr D. Dimitrov, for his valuable help in preparation of the figures.

REFERENCES

- [1] Antonucci, R. Unified models for active galactic nuclei and quasars. *Astron Astrophys* 1993; 31: 473-521.
- [2] Djorgowski SG, Volonteri M, Springel V, Bromm V, Meylan G. The origins and the early evolution of quasars and supermassive black holes. *Proceed. of XI Marcel Grossmann meeting on General Relativity*. Singapore: World Scientific 2008; p. 340.

- [3] Kembhavi AK, Narlikar JV. Quasars and active galactic nuclei: an introduction. Cambridge: Cambridge University Press 1999.
- [4] Lopez-Corredoira M. Pending problems in QSOs. *IJAA* 2011; 1(2): 73-82.
- [5] Lopez-Corredoira M. Observational cosmology: caveats and open questions in the standard model. *Recent Res Dev Astron Astrophys* 2003; 1: 567-1.
- [6] Greenstein JL, Schmidt M. The quasi-stellar radio sources 3C48 and 3C273. *Astrophys J* 1964; 140: 1-37.
- [7] Hoyle F, Fowler WA. Gravitational red-shifts in quasi-stellar objects. *Nature* 1967; 213: 373-4.
- [8] Das PK. Physical properties of collapsed objects with large central gravitational redshifts. *Mon Not R Aston Soc* 1976; 177: 391-408.
- [9] Narlikar JV. Two astrophysical applications of conformal gravity. *Ann Phys* 1977; 107: 325-36.
- [10] Narlikar JV, Arp HC. Flat spacetime cosmology - a unified framework for extragalactic redshifts. *Astrophys J* 1993; 405: 51-6.
- [11] Canalizo G, Stockton A. 3C48: stellar populations and the kinematics of stars and gas in the host galaxy. *Astrophys J* 2000; 528: 201-18.
- [12] Courbin F, Letawe G, Magain P, *et al.* On-axis spatially resolved spectroscopy of low redshift quasar host galaxies: HE1503+0228, at $z=0.135$. *Astron Astrophys* 2002; 394: 863-72.
- [13] Galianni P, Burbidge EM, Arp H, *et al.* The discovery of a high redshift X-ray emitting QSO very close to the nucleus of NGC7319. 2004 [Epub ahead of print].
- [14] Karlsson KG. Possible discretization of quasar redshifts. *Astron Astrophys* 1971; 13: 333-5.
- [15] Karlsson KG. On the existence of significant peaks in the quasar redshift distribution. *Astron Astrophys* 1977; 58: 237-40.
- [16] Burbidge G, Napier WM. The distribution of redshifts in new samples of quasi-stellar objects. *Astron J* 2001; 121: 21-30.
- [17] Arp H, Bi H, Chu Y, Zhu X. Periodicity of quasar redshifts. *Astron Astrophys* 1990; 239: 33-49.
- [18] Panov KP. Study of possible local quasars I: the first sample. *OAJ* 2011; 4: 14-26.
- [19] Arp HC. Catalogue of discordant redshift associations. Canada: APEIRON 2003.
- [20] Arp HC. Quasars, redshifts, and controversies. Berkeley, USA: Interstellar Medium 1987.
- [21] Burbidge G. The reality of anomalous redshifts in the spectra of some QSOs and its implications. *Astron Astrophys* 1996; 309: 9-22.
- [22] Burbidge GR. Noncosmological Redshifts. *Publ Astron Soc Pac* 2001; 113: 899-902.
- [23] Hoyle F, Burbidge G. Anomalous redshifts in the spectra of extragalactic objects. *Astron Astrophys* 1996; 309: 335-44.
- [24] Burbidge G, Hewitt A, Narlikar JV, Gupta PD. Associations between quasi-stellar objects and galaxies. *Astrophys J Suppl Ser* 1990; 74: 675-730.
- [25] Williams LLR, Irwin M. Angular correlations between LBQS and APM: weak lensing by the large-scale structure. *Mon Not R Aston Soc* 1998; 298: 378-88.
- [26] Bell MB. Further Evidence for Large Intrinsic Redshifts. *Astrophys J* 2002; 566: 705-11.
- [27] Jain B, Scranton R, Sheth RK. Quasar-galaxy and galaxy-galaxy cross-correlations: model predictions with realistic galaxies. *Mon Not R Aston Soc* 2003; 345: 62-70.
- [28] Lopez-Corredoira M, Gutierrez CM. Research on candidates for non-cosmological redshifts. USA: AIP Conf Proceed of First Crisis in Cosmology Conf 2006; vol. 822; pp. 75-96.
- [29] Burbidge G, Napier WM. Associations of High-Redshift Quasi-Stellar Objects with Active, Low-Redshift Spiral Galaxies. *Astrophys J* 2009; 706: 657-64.
- [30] Burbidge EM, Burbidge GR, Solomon PM, Strittmatter PA. Apparent associations between bright galaxies and quasi-stellar objects. *Astrophys J* 1971; 170: 233-40.
- [31] Sulentic JW, Arp HC. The galaxy-quasar connection: NGC4319 and Markarian 205. I Direct imagery. *Astrophys J* 1987; 319: 687-92.
- [32] Carilli CL, van Gorkom JH, Stocke J. 3C232 and NGC 3067: quasars, galaxies, and absorption lines. *Bull AAS* 1988; 20: 1027.
- [33] Carilli CL, van Gorkom JH, Stocke JT. Disturbed neutral hydrogen in the galaxy NGC3067 pointing to the quasar 3C232. *Nature* 1989; 338:134-6.
- [34] Arp H. A QSO 2.4 arcsec from a dwarf galaxy – the rest of the story. *Astron Astrophys* 1999; 341: L5-8.
- [35] Lopez-Corredoira M, Gutierrez CM. The field surrounding NGC7603: cosmological or non-cosmological redshifts? *Astron Astrophys* 2004; 421: 407-22.
- [36] Lopez-Corredoira M, Gutierrez CM. First tentative detection of anisotropy in the QSO distribution around nearby edge-on spiral galaxies. *Astron Astrophys* 2007; 461: 59-69.
- [37] Gosset E, Moreau O, Surdej J, *et al.* Surveys of ultraviolet-excess quasar candidates in large fields. *Astron Astrophys Suppl Ser* 1997; 123: 529-68.
- [38] Arp H. X-ray Observations of NGC1097 and nearby quasars. *Astrophys Space Sci* 1998; 262: 337-61.
- [39] Arp H, Burbidge EM, Chu Y, *et al.* NGC3628: Ejection activity associated with quasars. *Astron Astrophys* 2002; 391: 833-40.
- [40] Arp H, Burbidge EM, Carosati D. Quasars and galaxy clusters paired across NGC4410. 2006 [Epub ahead of print].
- [41] Burbidge EM, Burbidge G. QSOs in the field of the seyfert galaxy NGC5548. *Publ Astron Soc Pac* 2002; 114: 253-256.
- [42] Burbidge EM. Spectra of two quasars possibly ejected from NGC 4258. *Astron Astrophys* 1995; 298: L1-4.
- [43] Burbidge EM. Spectra of two x-ray emitting quasi-stellar objects apparently ejected from the Seyfert Galaxy NGC 2639. *Astrophys J* 1997; 484: L99-101.
- [44] Burbidge EM, Burbidge G. Ejection of matter and energy from NGC 4258. *Astrophys J* 1997; 477: L13-5.
- [45] Arp, H. Quasar creation and evolution into galaxies. *J Astrophys Astron* 1997; 18: 393-406.
- [46] Arp H, Burbidge EM, Chu Y, *et al.* NGC 3628: ejection activity associated with quasars. *Astron Astrophys* 2002; 391: 833-40.
- [47] Fan X, Narayanan VK, Lupton RH, *et al.* A survey of $z > 5.8$ quasars in the sloan digital sky survey I: discovery of three new quasars and the spatial density of luminous quasars at $z \sim 6$. *Astron J* 2001; 122: 2833-49.
- [48] Simon LE, Hamann FW, Pettini M. Physical properties of absorbers in high redshift quasars. *Rev Mex Astron Astrophys* 2007; 29: 177.
- [49] Maiolino R. Gas and dust in the most distant quasars. 2004; IAUS 222: 229-34.
- [50] Vermeulen RC, Cohen MH. Superluminal motion statistics and cosmology. *Astrophys J* 1994; 430: 467-94.
- [51] Zensus JA, Cohen MH, Unwin SC. The parsec-scale jet in quasar 3C345. *Astrophys J* 1995; 443: 35-53.
- [52] Burbidge G. NGC 6212, 3C345, and other quasi-stellar objects associated with them. *Astrophys J* 2003; 586: L119-22.
- [53] Bahcall JN, Kirhakos S, Saxe DH. Hubble space telescope images of a sample of 20 nearby luminous quasars. *Astrophys J* 1997; 479: 642-58.
- [54] McLure RJ, Kukula MJ, Dunlop JS, *et al.* A comparative HST imaging study of the host galaxies of radio-quiet quasars, radio-loud-quasars, and radio galaxies-I. *Mon Not R Aston Soc* 1999; 308: 377-404.
- [55] Di Matteo T, Springel V, Hernquist L. Energy input from quasars regulates the growth and activity of black holes and their host galaxies. *Nature* 2004; 433: 604-7.
- [56] Dunlop JS, McLure RJ, Kukula MJ, *et al.* Quasars, their host galaxies, and their central black holes. *Mon Not R Aston Soc* 2003; 340: 1095-135.
- [57] Grogin NA, Conselice CJ, Chatzichristou E, *et al.* AGN host galaxies at $z \sim 0.4 - 1.3$: Bulge – dominated and lacking merger – AGN connection. *Astrophys J* 2005; 627: L97-100.
- [58] Cattaneo A, Faber SM, Binney J, *et al.* The role of black holes in galaxy formation and evolution. *Nature* 2009; 460: 213-9.
- [59] Panov KP, Dimitrov DP. Study of possible local quasars II. A sample of 255 QSOs. Volume of contributions dedicated to Prof M. Contadakis, Thessaloniki, (in print).
- [60] Burbidge G. Two universes. *Astrophys Sp Sci* 1996; 244: 169-76.
- [61] Veron-Cetty MP, Veron P. A catalogue of quasars and active nuclei. 13th ed. *Astron Astrophys* 2010; 518A: A10.
- [62] Croom SM, Smith RJ, Boyle BJ, *et al.* The 2dF QSO Redshift Survey –V. The 10k catalogue. *Mon Not R Aston Soc* 2001; 322: L29-36.
- [63] Arp H, Surdej J, Swings J-P. Two quasars seen near the spiral galaxy NGC 470. *Astron Astrophys* 1984; 138:179-82.
- [64] Arp H, Duhalde O. Quasars near NGC 520. *Publ Astron Soc Pac* 1985; 97: 1149-57.

- [65] Arp H. Quasars associated with NGC 613, NGC 936 and NGC 941. *Astrophys Space Sci* 2006; 301:117-26.
- [66] Arp H, Roscoe D, Fulton C. Periodicities of quasar redshifts in large area surveys. NY: BKS Press 2005.
- [67] Abazajian K, Adelman-McCarthy JK, *et al.* The second data release of the sloan digital sky survey. *Astron J* 2004; 128: 502-12.
- [68] Burbidge EM. A group of quasi-stellar objects closely associated with NGC 1068. *Astrophys J* 1999; 511: L9-L11.
- [69] Arp H, Sulentic JW. Three quasars near the spiral arms of NGC 1073. *Astrophys J* 1979; 229: 496-502.
- [70] Kaaret P. Optical Sources near the bright X-Ray Source in NGC 1073. *Astrophys J* 2005; 629: 233-8.
- [71] Arp H. Pairs of X-ray sources across Seyferts: the NGC 4235 field. *Astron Astrophys* 1997; 328: L17-L20.
- [72] Arp H. Further Observations and Analysis of Quasars near Companion Galaxies. *Astrophys J* 1983; 271: 479-506.
- [73] Arp H. Quasars near companion galaxies. *Astrophys J* 1981; 250: 31-42.
- [74] Arp H. High – redshift objects near the companion galaxies to NGC 2859. *Astrophys J* 1980; 240: 415-20.
- [75] Burbidge EM, Burbidge G, Arp HC, Zibetti S. QSOs associated with M82. *Astrophys J* 2003; 591: 690-4.
- [76] Burbidge EM, Burbidge G, Arp HC, Napier WM. An anomalous concentration of QSOs around NGC 3079. *Astrophysics* 2005 [Epub ahead of print].
- [77] Arp H, Sulentic JW, di Tullio G. Quasars aligned across NGC 3384. *Astrophys J* 1979; 229: 489-95.
- [78] Chu Y, Wei J, Hu J, *et al.* Quasars around the Seyfert Galaxy NGC 3516. *Astrophys J* 1998; 500: 596-8.
- [79] Arp H. Two newly discovered quasars closely spaced across a galaxy. *Astrophys J* 1984; 283: 59-63.
- [80] Arp H, Gavazzi G. A third quasar close to NGC 3842. *Astron Astrophys* 1984; 139: 240-2.
- [81] Zhu X, Chu Y, Wei J, *et al.* A quasar possibly ejected from NGC 4579. *Chin Sci Bull* 2000; 45: 886-8.
- [82] Arp H, Russell D. A possible relationship between quasars and clusters of galaxies. *Astrophys J* 2001; 549: 802-19.
- [83] Arp HC, Burbidge EM, Chu Y, Zhu X. X-Ray emitting QSOs ejected from Arp 220. *Astrophys J* 2001; 553: L11-3.
- [84] Arp H. The surroundings of disturbed, active galaxies. *Astrophys J* 2001; 549: 780-801.
- [85] Weedman DW. A photometric study of markarian galaxies. *Astrophys J* 1973; 183: 29-39.
- [86] Arp H, Fulton C. A cluster of high redshift quasars with apparent diameter 2.3 degrees. ArXiv 2008 [Epub ahead of print].
- [87] Ambartsumian VA. La structure et l'évolution de l'univers. 11th ed. Bruxelles: Conseil de Physic Solvay 1958.
- [88] Arp H. Evolution of quasars into galaxies and its implications for the birth and evolution of matter. *APEIRON* 1998; 5: 135-42.

Received: February 18, 2013

Revised: May 08, 2013

Accepted: May 08, 2013

© Kiril P. Panov; Licensee *Bentham Open*.

This is an open access article licensed under the terms of the Creative Commons Attribution Non-Commercial License (<http://creativecommons.org/licenses/by-nc/3.0/>) which permits unrestricted, non-commercial use, distribution and reproduction in any medium, provided the work is properly cited.